

FERROMAGNETIC RESONANCE IN POLYCRYSTALLINE FERRITES

PROEFSCHRIFT

TER VERKRIJGING VAN DE GRAAD VAN DOCTOR IN DE
TECHNISCHE WETENSCHAP AAN DE TECHNISCHE HOGE-
SCHOOL TE DELFT, KRACHTENS ARTIKEL 2 VAN HET
KONINKLIJK BESLUIT VAN 16 SEPTEMBER 1927, STAATS-
BLAD NR 310, EN OP GEZAG VAN DE RECTOR MAGNI-
FICUS DR. O. BOTTEMA, HOOGLERAAR IN DE AFDELING
DER ALGEMENE WETENSCHAPPEN, VOOR EEN COM-
MISSIE UIT DE SENAAT TE VERDEDIGEN OP WOENS-
DAG 4 JUNI 1958 DES NAMIDDAGS TE 2 UUR DOOR

JAN SNIEDER

GEBOREN TE EDAM



'S-GRAVENHAGE
MARTINUS NIJHOFF
1958

1012 ~~BTRH~~ A40

Dit proefschrift is goedgekeurd door de promotor

Prof. Dr. R. KRONIG

AAN MIJN OUDERS

Voor het onderzoek, beschreven in dit proefschrift mocht gebruik worden gemaakt van de faciliteiten van het Fysisch Laboratorium der Rijksverdedigingsorganisatie T.N.O. Aan het Bestuur van de Rijksverdedigingsorganisatie, dat mij toestemming heeft willen verlenen tot het publiceren van de resultaten van dit onderzoek, betuig ik mijn hartelijke dank.

CONTENTS

CHAPTER I. INTRODUCTION

CHAPTER II. THE PHENOMENOLOGICAL DESCRIPTION OF THE HIGH FREQUENCY MAGNETIC BEHAVIOUR OF FERRITES

§ 1.	The permeability tensor.	11
§ 2.	Propagation of electromagnetic waves in round wave guides containing a concentric round ferromagnetic rod	12
§ 3.	Faraday rotation and ellipticity	14

CHAPTER III. EXPERIMENTAL ARRANGEMENTS

§ 4.	The materials used and their preparation.	15
§ 5.	Electronic equipment for the study of the Faraday effect in rods of ferrite.	16
§ 6.	The solenoid and its magnetic field	18
§ 7.	Arrangement for measuring the magnetization of the rods	19
§ 8.	Equipment for regulating and measuring the temper- ature	20
§ 9.	Electronic equipment for the study of resonance in spherical probes of ferrite	20

CHAPTER IV. THE EXPERIMENTAL RESULTS

§ 10.	Faraday rotation and ellipticity measurements on ferrite rods	22
§ 11.	Sources of error in the rotation and ellipticity measure- ments.	28
§ 12.	Measurements of the magnetization.	29

§ 13. Resonance measurements on ferrite spheres	29
§ 14. Sources of error in the resonance measurements.	32

CHAPTER V. INTERPRETATION OF THE ROTATION AND
ELLIPTICITY MEASUREMENTS IN TERMS OF FERROMAG-
NETIC RESONANCE

§ 15. The permeability tensor.	35
§ 16. Ferromagnetic resonance in spheres.	38
§ 17. Determination of the damping constant α from the rotation and ellipticity measurements	39

CHAPTER VI. THE INFLUENCE OF POROSITY ON THE
RESONANCE CONDITIONS

§ 18. Outline of the problem	44
§ 19. The influence of porosity on the g -value	45

CHAPTER VII. THE INFLUENCE OF POROSITY ON THE
LINE WIDTH

§ 20. Outline of the problem	51
§ 21. Estimate of the line width.	52
§ 22. The damping constant α	55

FERROMAGNETIC RESONANCE IN POLYCRYSTALLINE FERRITES

Summary

An experimental and theoretical study is made of the propagation of TE_{11} -waves of wavelength 3.2 cm in a round wave guide containing a concentric round rod of Ferroxcube IV magnetized by a static magnetic field in a longitudinal direction. The Faraday rotation and the ellipticity when the wave has passed a given length of rod is determined as a function of the static field strength through resonance and of the temperature over a range from -30 to 100°C . On the basis of the theory of ferromagnetic resonance with damping the elements of the gyromagnetic permeability tensor are computed. With them the rotation angle and ellipticity can be expressed in terms of the angular frequency of the wave, the radius of the wave guide, the radius and length of the rod, the static field strength, the static magnetization, the gyromagnetic ratio and the damping constant. The gyromagnetic ratio is determined from resonance measurements on spheres of Ferroxcube while the damping constant is chosen so as to give the best agreement between theory and experiment. An interpretation of the values of the gyromagnetic ratio and of the resonance width in terms of the porosity of the ferrites is given. The behaviour of the damping constant as a function of porosity is briefly discussed.

CHAPTER I. INTRODUCTION

The purpose of the present investigation is on the one hand the experimental determination of a number of quantities which are characteristic for the behaviour of various ferromagnetic ferrites under the influence of high frequency electromagnetic fields, and on the other hand the interpretation of the data thus obtained in terms of the theory of ferromagnetic resonance.

In Chapter II the phenomenological description of ferromagnetic

materials in the simultaneous presence of a static and a high frequency magnetic field with the aid of a gyromagnetic permeability tensor is briefly summarized. The possibility of losses is explicitly taken into account. With a view to the experiments to be described in Chapter III the theory governing the propagation of electromagnetic waves in a round wave guide, containing a concentric round rod of ferromagnetic material under the influence of a static longitudinal magnetic field, is gone into in greater detail. By generalizing earlier work of van Trier¹⁾ a relation expressing the rotation of the plane of polarization and ellipticity of a TE_{11} -wave, after traversing a given length of the guide, in terms of the permeability tensor of the ferromagnetic material is given.

In Chapter III two kinds of experimental arrangements are described. In the first of these the rotation of the plane of polarization and the ellipticity referred to above can actually be measured at a wavelength of 3.2 cm, for a static longitudinal magnetic field ranging from 0 to 5×10^5 A/m and at a temperature between -40 and 120°C . The second arrangement serves to study the absorption of high frequency electromagnetic energy in small spheres of the materials investigated, contained in a cavity, for three frequencies, corresponding to wavelengths of 3.2, 1.6 and 1.25 cm, as a function of a static magnetic field ranging up to 8×10^5 A/m and of the temperature in the interval already mentioned. By varying the magnetic field the value can be found for which the absorption is a maximum, corresponding to resonance. The ratio of the angular frequency and the field strength at resonance is the so-called gyromagnetic ratio of the material.

In Chapter IV the experimental results are collected both for the rotation and the resonance experiments. Several sources of error which may affect the measurements are discussed, together with the precautions necessary to avoid them. The degree of accuracy of the measured values is also estimated here.

In Chapter V the theory of ferromagnetic resonance with a damping term in the fundamental equation is reviewed. The elements of the gyromagnetic permeability tensor introduced in Chapter II are computed from this theory for a ferromagnetic medium in the presence of a static magnetic field and in the case that magnetic saturation is completely or almost completely attained. They can be expressed in terms of the gyromagnetic ratio, the damping

constant, the angular frequency, the static field strength and the static magnetization. After a survey of ferromagnetic resonance in spheres, the theoretical values of the elements of the permeability tensor are substituted into the expressions derived in Chapter II for the rotation angle and ellipticity of a TE_{11} -wave traversing a longitudinally magnetized ferrite rod in a round wave guide. By choosing a suitable value of the unknown damping constant, the theoretical curves can be made to conform to the experimental curves. In this way the damping constant can be determined for the various ferrites as a function of the temperature. The temperature dependence is found to be relatively slight, but there appears a strong influence of the porosity, in the sense that the greater the porosity the larger the damping constant. Using the damping constant giving the best fit, the computed values of the resonance field strength are compared with the observed ones, extrapolated to vanishing radius of the rods. A reasonable agreement is found.

In Chapter VI it is investigated why the gyromagnetic ratio as determined from resonance measurements on small spheres of the same ferrites used in the rotation experiments has values depending on the temperature and on the wavelength. It is shown that the inhomogeneity of the material arising from its porous structure accounts essentially for this dependence.

The porosity of the ferrites is accompanied by an inhomogeneity of the static field inside the material. As a consequence a broadening of the resonance frequency takes place in addition to broadening due to other causes. In Chapter VII an estimate of the width due to porosity is made under some simplifying assumptions and compared with experiment. We also give a brief discussion of the mechanism operative in ferromagnetic damping as manifested in the ferromagnetic damping constant and its dependence on porosity.

CHAPTER II. THE PHENOMENOLOGICAL DESCRIPTION OF THE HIGH FREQUENCY MAGNETIC BEHAVIOUR OF FERRITES

§ 1. *The permeability tensor.* If in an isotropic ferromagnetic material, or one which by reason of its polycrystalline structure may be considered as isotropic, a static magnetic field H_0 is applied, then, as discussed e.g. in the thesis of van Trier¹⁾, the reaction of this material to a high frequency magnetic field can suitably be

described by a gyromagnetic permeability tensor of the form

$$\|\mu\| = \begin{vmatrix} \mu_1 & -j\mu_2 & 0 \\ j\mu_2 & \mu_1 & 0 \\ 0 & 0 & \mu_3 \end{vmatrix}, \quad (2.1)$$

relating the components of the high frequency part of the magnetic induction \mathbf{B} to the components of the high frequency part of the magnetic field strength \mathbf{H} . In the thesis of van Trier, who was concerned with the behaviour far below resonance, μ_1 , μ_2 and μ_3 were considered as real quantities, signifying the absence of magnetic losses. Here we shall take into account from the beginning the possibility of such losses, and we shall hence assume μ_1 , μ_2 and μ_3 to be complex:

$$\mu_1 = \mu_1' - j\mu_1'', \mu_2 = \mu_2' - j\mu_2'', \mu_3 = \mu_3' - j\mu_3'', \quad (2.2)$$

where μ_1' , μ_1'' , μ_2' , μ_2'' , μ_3' , μ_3'' are real. These quantities will depend on the kind of material, the value of H_0 , the temperature T and the angular frequency ω of the alternating field. Following van Trier we assume the dielectric behaviour of the ferrites to be describable by one dielectric constant

$$\varepsilon = \varepsilon' - j\varepsilon'', \quad (2.3)$$

independent of direction, which, however, in contrast to him we also allow to be complex.

§ 2. *Propagation of electromagnetic waves in round wave guides containing a concentric round ferromagnetic rod.* We consider now a round wave guide with a wall that may be regarded as perfectly conducting, containing a concentric round rod of a ferromagnetic ferrite which can be characterized by a gyromagnetic permeability tensor (2.1), (2.2) and a dielectric constant (2.3) as discussed in § 1. In particular we give our attention to a TE_{11} -mode in the empty wave guide and the changes in its propagation arising from the presence of a ferrite rod with radius ρ_1 very much smaller than the radius ρ_0 of the wave guide. The TE_{11} -mode in the empty guide may be resolved into two circularly polarized modes, depending on the azimuth ϑ around the axis of the guide through the factor $\exp(\pm j\vartheta)$.

As shown by van Trier the propagation constant $\gamma_0 = j\beta_0$ of the TE_{11} -mode (which is purely imaginary since in the empty guide

no losses occur) is altered in a different way for the two circularly polarized modes by the introduction of the rod, becoming (see his equation (2.118))

$$\gamma_{\pm} = \gamma_0 - c_1 \gamma_0 \left(\frac{\mu_1 \pm \mu_2 - \mu_0}{\mu_1 \pm \mu_2 + \mu_0} + c_2 \frac{\varepsilon - \varepsilon_0}{\varepsilon + \varepsilon_0} \right) \rho_1^2. \quad (2.4)$$

Here the constants c_1 and c_2 are given by

$$c_1 = \frac{\pi \sigma_0 N_1'(\sigma_0 \rho_0)}{4 \rho_0 J_1''(\sigma_0 \rho_0)}, \quad c_2 = - \frac{\omega^2 \varepsilon_0 \mu_0}{\gamma_0^2}, \quad (2.5)$$

with ε_0 , μ_0 the dielectric constant and permeability of vacuum, σ_0 follows from $J_1'(\sigma_0 \rho_0) = 0$ as first root, γ_0 from

$$\gamma_0^2 = \sigma_0^2 - \omega^2 \varepsilon_0 \mu_0, \quad (2.6)$$

and N_1 and J_1 are the Neumann- and Besselfunctions of order 1, the primes denoting differentiation with respect to the argument. By an approximation method in which they started from an empty wave guide and computed the first order perturbation produced by the presence of the thin rod Suhl and Walker²⁾ could confirm the result of van Trier.

As was mentioned before, van Trier was primarily interested in the practically lossless case at frequencies far below resonance. It appears, however, that his derivation applies unchanged in case μ_1 , μ_2 , μ_3 and ε are complex as supposed in (2.2) and (2.3). As a consequence of (2.4) γ_{\pm} will then also be complex. Writing

$$\gamma_{\pm} = \alpha_{\pm} + j\beta_{\pm} \quad (2.7)$$

and equating real and imaginary parts in (2.7) and (2.4) we find

$$\alpha_{\pm} = 2c_1 \beta_0 \left[\frac{\mu_0(\mu_1'' \pm \mu_2'')}{(\mu_1' \pm \mu_2' + \mu_0)^2 + (\mu_1'' \pm \mu_2'')^2} + c_2 \frac{\varepsilon_0 \varepsilon''}{(\varepsilon' + \varepsilon_0)^2 + \varepsilon''^2} \right] \rho_1^2, \quad (2.8)$$

$$\beta_{\pm} = \beta_0 - c_1 \beta_0 \left[\frac{(\mu_1' \pm \mu_2')^2 - \mu_0^2 + (\mu_1'' \pm \mu_2'')^2}{(\mu_1' \pm \mu_2' + \mu_0)^2 + (\mu_1'' \pm \mu_2'')^2} + c_2 \frac{\varepsilon'^2 - \varepsilon_0^2 + \varepsilon''^2}{(\varepsilon' + \varepsilon_0)^2 + \varepsilon''^2} \right] \rho_1^2. \quad (2.9)$$

§ 3. *Faraday rotation and ellipticity.* The electric fields of the two circularly polarized components originally constituting the TE₁₁-wave in their dependence on the time t , the coordinate z measured along the guide in the direction of propagation and the azimuth ϑ around the axis of the guide, can be written as

$$\begin{aligned}\mathbf{E}_+ &= \hat{\mathbf{E}}_+ \exp(-\alpha_+ z) \exp j(\omega t + \vartheta - \beta_+ z), \\ \mathbf{E}_- &= \hat{\mathbf{E}}_- \exp(-\alpha_- z) \exp j(\omega t - \vartheta - \beta_- z),\end{aligned}\quad (2.10)$$

\mathbf{E}_+ , \mathbf{E}_- , $\hat{\mathbf{E}}_+$, $\hat{\mathbf{E}}_-$ being perpendicular to the axis of the guide. Let us assume that for $z = 0$ we have equal amplitudes so that $\hat{\mathbf{E}}_+ = \hat{\mathbf{E}}_- = \hat{\mathbf{E}}$. The result of the superposition of the two expressions (2.10) can then be written as

$$\begin{aligned}\mathbf{E} = \mathbf{E}_+ + \mathbf{E}_- &= 2\hat{\mathbf{E}} \exp[-\frac{1}{2}(\alpha_+ + \alpha_-)z] \exp j[\omega t - \frac{1}{2}(\beta_+ + \beta_-)z] \\ &\cdot \{ \cosh[-\frac{1}{2}(\alpha_+ - \alpha_-)z] \cos[\vartheta - \frac{1}{2}(\beta_+ - \beta_-)z] + \\ &+ j \sinh[-\frac{1}{2}(\alpha_+ - \alpha_-)z] \sin[\vartheta - \frac{1}{2}(\beta_+ - \beta_-)z] \}.\end{aligned}\quad (2.11)$$

From the factor in brackets $\{ \}$ in (2.11) it appears that for a given z the vector \mathbf{E} consists of two components, 90° out of phase in time, the first of which has its maximum value for $\vartheta = \frac{1}{2}(\beta_+ - \beta_-)z$, the second for $\vartheta = \frac{1}{2}(\beta_+ - \beta_-)z + \frac{1}{2}\pi$. We see thus that on passing through a distance z the direction of maximum \mathbf{E} for both components turns through an angle

$$\vartheta = \frac{1}{2}(\beta_+ - \beta_-)z. \quad (2.12)$$

The rotation over unit distance

$$\Theta = \frac{1}{2}(\beta_+ - \beta_-) \quad (2.13)$$

is called the Faraday rotation. The ratio of the maximum values of the two components is suitably called the ellipticity and is according to (2.11) given by

$$\eta = \coth \frac{1}{2}(\alpha_+ - \alpha_-)z. \quad (2.14)$$

By means of (2.8), (2.9), (2.5) and (2.6) ϑ and η as given by (2.12) and (2.14) can be expressed in terms of the elements of the gyromagnetic permeability tensor and the dielectric constant of the ferromagnetic material, together with the angular frequency ω , the propagation constant γ_0 of the empty guide and the radii ρ_0 and ρ_1 of guide and rod.

From substitution of (2.8) and (2.9) in (2.12) and (2.14) it appears that due to cancellation of terms the dielectric behaviour does not enter into the quantities ϑ and η .

CHAPTER III. EXPERIMENTAL ARRANGEMENTS

§ 4. *The materials used and their preparation.* The materials studied were the same as those used by van Trier¹⁾, viz. Ferroxcube IV, A, B, C, D, E, prepared at the Philips Laboratories in Eindhoven. They are nickel zinc ferrites with nickel and zinc in different proportions, produced by a sintering process which gives rise to a certain porosity. We repeat in table I the data on the chemical composition, specific gravity and porosity which have already been given by van Trier.

TABLE I

Ferroxcube	Chemical composition in mol %		Specific gravity	Porosity %
	NiO	ZnO		
IV A	17.5	33.2	4.45	16.6
IV B	24.9	24.9	4.80	11.0
IV C	31.7	16.5	4.52	16.2
IV D	39.0	9.4	3.98	26.2
IV E	48.2	0.7	3.80	29.5

In the Faraday rotation experiments the rods of ferrite were the ones investigated by van Trier. The method of their preparation has been described by him in detail.

The ferrite spheres for the resonance absorption experiments were obtained as follows. Samples of roughly equal dimensions in all three directions were cut from the material. These samples were placed into a vertical cylinder, the side wall of which was covered on the inside with emery paper. The bottom of the cylinder was closed, the top contained an orifice covered with gauze, permitting the passage of air. The samples were introduced into the cylinder and by means of a strong air jet, blown tangentially into the cylinder through the side wall, were violently thrown about, finally obtaining a spherical shape. On continuing the process the spheres could be ground down to smaller diameters. By observing the rolling of the spheres on a slightly inclined plane glass plate their roundness

could be checked, imperfections manifesting themselves by deviations from rectilinear motion.

§ 5. *Electronic equipment for the study of the Faraday effect in rods of ferrite.* Fig. 1 represents the apparatus employed in the form of a block diagram. The klystron was of the type 723 A/B, working in the 3 cm-band. The electromagnetic wave emitted passed a wavemeter, furnishing the frequency, a calibrated variable attenuator and a uniline which provided the decoupling of the klystron. The wave then entered a rectangular wave guide of such dimensions that only the TE_{01} -mode can be propagated. This wave guide gradually changed over into a round wave guide, called the rotator, in which the TE_{01} -mode becomes a TE_{11} -mode. The round

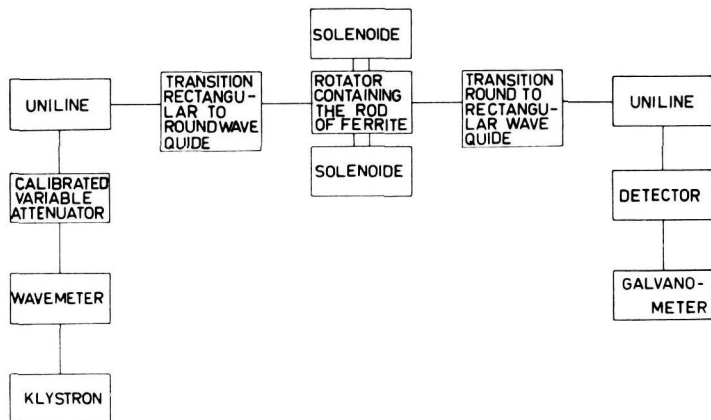


Fig. 1. Block diagram of the Faraday rotation equipment.

wave guide was composed of two identical parts which could be rotated with respect to each other around their common axis. The second part changed continuously into a rectangular guide of the same dimensions as the one preceding the first part, bearing a crystal detector at its end. The detector is connected to a galvanometer. The angle through which the second part of the rotator was turned with respect to the first part could be read on a scale.

In each part of the rotator near its outward end a plate of conducting material (paper covered with carbon black) through the axis and parallel to the long side of the attached rectangular wave guide was present. This plate absorbed any component wave of

which the plane of polarization coincided with it, the component wave polarized perpendicular to the plate not suffering any damping.

In the middle of the rotator along its axis the rods of ferrite to be investigated were situated. They were supported by a wedge of (rigid) foam plastic attached to the inside of a hollow cylinder of the same material which was then introduced into the guide as shown in fig. 2. In mounting the rod on the wedge care was taken by means of a special metal fitting to place the rod precisely in a concentric position. The electromagnetic behaviour of the foam plastic is identical with that of air (or of free space) within the accuracy of our measurements. The method of supporting the rod was so chosen as to have a free channel along it through which air could be passed. By pre-cooling or pre-heating the air current the temperature of the rod could be varied. A solenoid around the rotator could furnish a longitudinal magnetic field. The construction and the field of this solenoid will be considered in § 6.

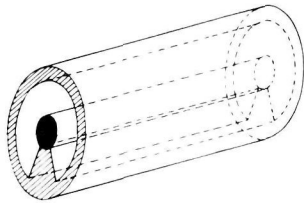


Fig. 2. Attachment of the ferrite rod to the foam plastic cylinder.

Before the rod was introduced into the rotator, the zero reading of the rotator scale could be determined by turning the second half into such a position that a maximum signal was read on the galvanometer. The position 90° further on where the signal is a minimum could be fixed still more accurately because for it the power entering the rotator could be chosen larger, giving a big deflection of the galvanometer already for small deviations from the minimum position. After the rod had been introduced, it was first demagnetized by an alternating current through the solenoid. Then the rotation angle to which the rod gave rise when a static magnetic field was generated parallel to it by means of a direct current through the solenoid could be measured by finding the new position of minimum reading.

With the aid of the variable calibrated attenuator we could determine the intensity ratio for the positions of maximum and minimum reading and thus the square of the ellipticity, conveniently expressed in decibels. Similarly by measuring the intensity ratio for the empty guide and the guide containing the magnetized ferrite rod for the position of maximum reading we could obtain the insertion loss in decibels.

§ 6. *The solenoid and its magnetic field.* The static magnetic field to be applied to the ferrite rod in the rotator was produced by a solenoid consisting of two separate parts which were placed end to end as shown in fig. 3, where also the dimensions are indicated. The

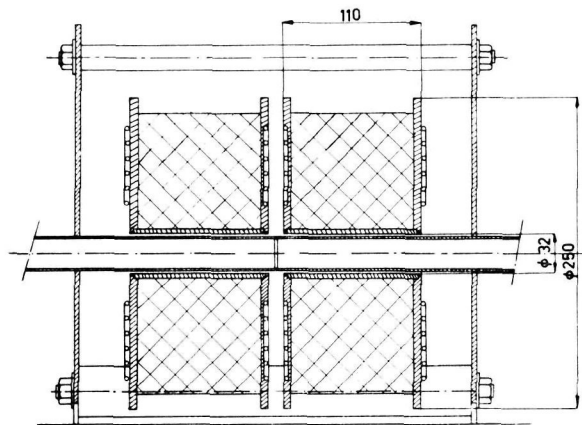


Fig. 3. Watercooled solenoids for the Faraday rotation experiments.
Distances in mm.

end plates of each part, made of brass, were joined by a brass cylinder. They were water-cooled, no further cooling being used. The windings of insulated copper wire, 3 mm in diameter, were placed around the cylinder without additional insulation. A thermocouple, introduced in the region of the coils which became warmest, allowed to measure the temperature there.

The magnetic field strength along the axis of the solenoid was measured by turning a small test coil quickly through 180° from a parallel into an antiparallel position and by taking the reading of a ballistic galvanometer connected to it. The scale of the galvanometer had been calibrated with magnetic fields of known strength,

very accurately determined by means of proton-resonance. Fig. 4 represents the axial field strength for a current of 12 A through the windings along the central 12 cm of the pair of solenoids when in an adjacent position.

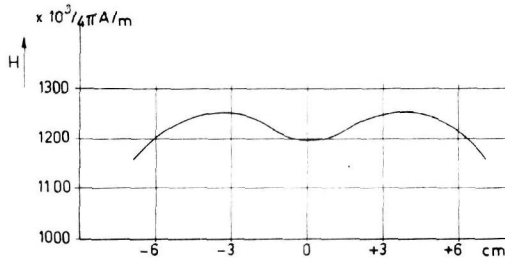


Fig. 4. Axial field strength in the solenoid of fig. 3 at a current of 12A.

The field strength could be varied continuously from 0 to 5×10^5 A/m. At the higher values the time available for measurements was limited by the heating of the coils. With a view to the insulation a maximum temperature of 120°C was permissible.

By separating the solenoids and introducing iron cores inside, fairly homogeneous magnetic fields of considerably greater strength could be produced in a limited region between the end surfaces of these cores.

§ 7. *Arrangement for measuring the magnetization of the rods.* In connection with the theoretical interpretation of the Faraday rotation and ellipticity observed in our experiments on ferrite rods a knowledge of the magnetization produced by the static magnetic field is required. The arrangement for determining this consisted of two short coils in series with a galvanometer. The two coils were identical, except in being wound in opposite direction. In each of the two parts of the solenoid described in § 6 one coil was placed coaxially at the centre, the two parts being sufficiently separated from each other so that no magnetic coupling between the coils occurred. If the same current was passed through the two parts of the solenoid, then on varying this current or on reversing its direction the galvanometer did not show a deflection by reason of the opposite sense of winding of the coils.

On introducing a ferrite rod into one of the coils an additional flux proportional to the magnetization of the rod passed through this coil, and when the current through the parts of the solenoid was reversed, a deflection of the galvanometer was caused. Repeating the procedure with a nickel rod of the same dimensions as the ferrite rod, the ratio of the galvanometer deflections gave the ratio of the magnetizations in the two cases. From the known magnetic properties of nickel³⁾ the magnetization of the ferrite rod could then be computed.

§ 8. *Equipment for regulating and measuring the temperature.* For measurements above room temperature the air that passes the ferrite rod through the channel in the foam plastic mounting mentioned in § 5 was pumped through the interspace between two concentric tubes, on the inner one of which an electrically heated spiral was wound. By adjusting the heating current of the spiral and the speed of the air, the temperature could be varied from room temperature to about 150°C, the softening point of the solder connecting the sections of the wave guide. For measurements below room temperature the air was pumped through a helical tube in a heat exchanger connected to a frigidaire cooling-machine. The temperature of the cold air could either be varied by changing its speed or by admixing air of room temperature, the temperature range being from -40°C to room temperature.

The temperature of the ferrite rods in the rotator was measured with two calibrated constantan-copper thermocouples, one placed at the entrance, the other at the exit of the rotator. The average of the two temperatures was taken as the temperature of the rod. This procedure was justified by some test-runs in which a third thermocouple was placed next to the rod near its centre.

§ 9. *Electronic equipment for the study of resonance in spherical probes of ferrite.* The electronic set-up for the measurements in question is shown diagrammatically in fig. 5. The klystron was sawtooth-modulated in its repeller tension. The modulated signal passed a wavemeter, a variable attenuator and a uniline, arriving in the magic tee. One of the other guides of this magic tee was closed by a shortcircuit piston, the other two were respectively connected to a crystal detector and a half-wavelength cavity. The coupling

of this cavity to the guide was achieved by means of a coupling hole. The small sphere to be studied was supported in the cavity on a slab of foam plastic in such a position that the high frequency magnetic and electric field there had a maximum value and the value zero respectively. The static magnetic field could be applied to the cavity by means of the solenoid already described in § 6. Without this field the mode of the klystron appeared on the oscilloscope when its base was modulated in the same way as the klystron.

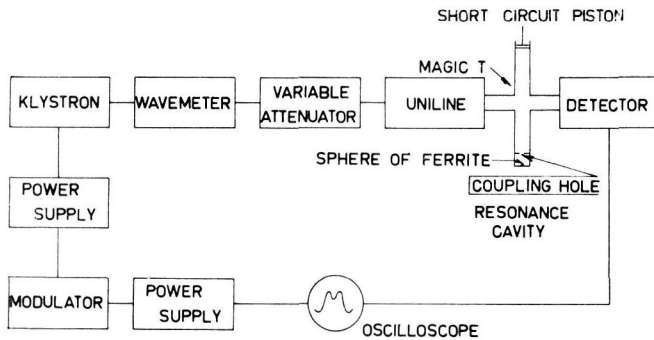


Fig. 5. Block diagram of the resonance equipment for measurements on spheres.

When in the absence of a static magnetic field the frequency was adjusted so as to make half the wavelength equal to the length of the cavity, a dip could be seen in the mode of the klystron which is due to the absorption of the cavity. Care was taken to have this dip at the centre of the mode on the oscilloscope. On gradually applying the static magnetic field in a direction perpendicular to that of the high frequency magnetic field at first a decrease of the dip and a shift to one side were observed as ferromagnetic resonance in the sphere was approached. Indeed, under these conditions the presence of the sphere will noticeably alter the resonance frequency of the cavity as well as its quality factor. On increasing the static field the dip attained a minimum value, at the same time returning to its original position. On still further increasing the static field the dip passed to the other side and gradually increased again. The minimum of the dip corresponds to the maximum of ferromagnetic resonance absorption.

The value of the static magnetic field at which this occurs will be denoted by H_r . By the relation

$$\omega = \Gamma H_r, \quad (3.1)$$

where ω is the angular frequency of the wave used, as determined by the wavemeter, we can introduce the gyromagnetic ratio Γ which thus can be found experimentally.

Measurements similar to the ones described could be performed with a transmission cavity having a coupling hole at either end and replacing the magic tee in fig. 5. The length of the cavity must be an integral number of half wavelengths. Actually it was equal to one wavelength. The procedure was otherwise the same as in the previous case.

It should be noted that the dielectric behaviour of the sphere was immaterial for the resonance phenomenon discussed. In the first place this behaviour is not influenced by a static magnetic field, but besides, as already stated, the position of the sphere in our measurements was so chosen as to make the high frequency electric field near it practically zero.

CHAPTER IV. THE EXPERIMENTAL RESULTS

§ 10. *Faraday rotation and ellipticity measurements on ferrite rods.* With the electric equipment described in §§ 5 and 6 the Faraday rotation and ellipticity produced in the TE_{11} -wave of a round wave guide by concentric ferrite rods of length $l = 3.45$ cm as mentioned in § 4 were investigated at a wavelength $\lambda = 3.2$ cm and as a function of the static longitudinal magnetic field H_0 , for various radii ρ_1 of the rods and at three temperatures $T = -32^\circ\text{C}$, room temperature ($20-22^\circ\text{C}$), 120°C .

In figs 6-11 the results for the dependence on H_0 at room temperature are represented for rods of the various kinds of ferrite, having respectively radii of 0.5 (in case of rod IV C this was 0.6), 1.0 and 1.5 mm. Figs 6, 8 and 10 show the rotation angle ϑ as defined in § 3 in degrees, figs 7, 9 and 11 the ellipticity η , or more precisely $20_{10} \log \eta$ in decibels. In the last three figures the insertion loss as discussed in § 5, i.e. the intensity ratio at the position of maximum reading for the empty guide and the guide containing the magnetized

rod, is also given, expressed in decibels. Actually this intensity ratio was found by first measuring once and for all the ratio for the empty guide and the guide containing the demagnetized rod, and thereupon the ratio for the guide containing the demagnetized rod and the guide containing the magnetized rod.

From these figures we see at once that the value of H_0 at which the curve for the Faraday rotation crosses the axis ($\vartheta = 0$) in all cases is the same (within the accuracy of the curves) as the value

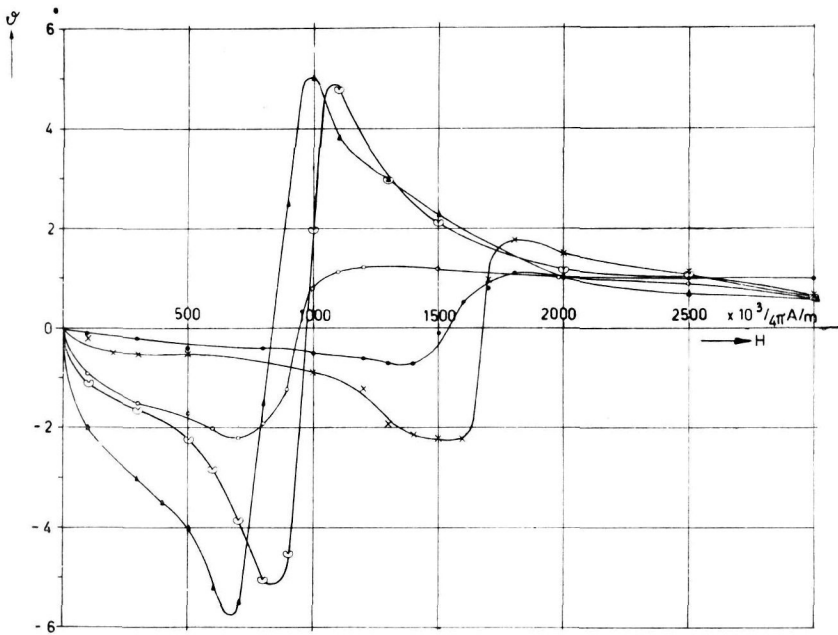


Fig. 6. The rotation angle ϑ vs. the static magnetic field strength H_0 for rods of the ferrites A(\times), B(∞), C(Δ), D(\odot), E(.) at a wavelength $\lambda = 3.2$ cm and a temperature $T = 22^\circ\text{C}$. Length of the rods $l = 3.5$ cm, radius $\rho_1 = 0.05$ cm for A, B, D and E and 0.06 cm for C.

at which the ellipticity curve for the same rod has a minimum. This is also true for the other temperatures, -32°C and 120°C , for which the curves have not been included here since they are of the same type as those of figs 6-11. We may hence call this value H_r of H_0 the effective resonance value.

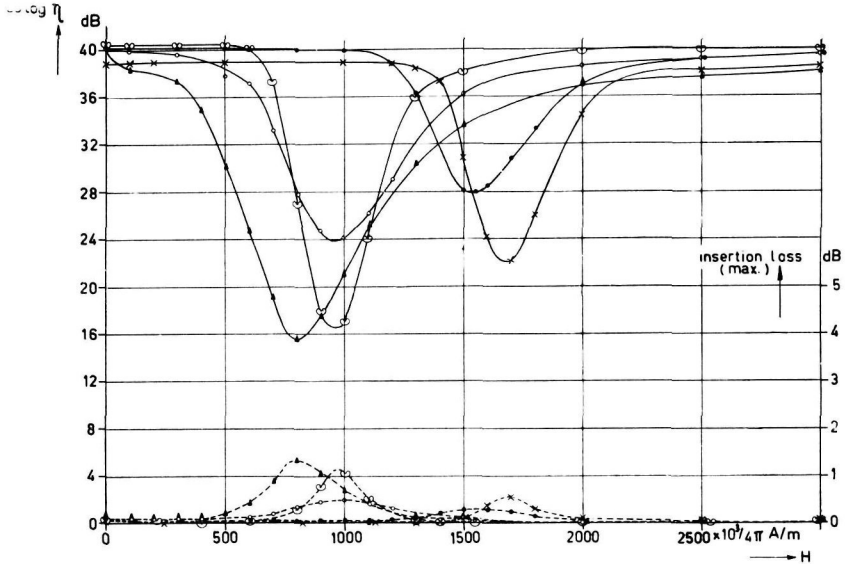


Fig. 7. The measured ellipticity vs. the static magnetic field strength H_0 for rods of the ferrites A(\times), B(∞), C(Δ), D(\circ) and E(\cdot) at a wavelength $\lambda = 3.2$ cm and a temperature $T = 22^\circ\text{C}$. Length of the rods $l = 3.5$ cm, radius $\rho_1 = 0.05$ cm for A, B, D and E and 0.06 cm for C.

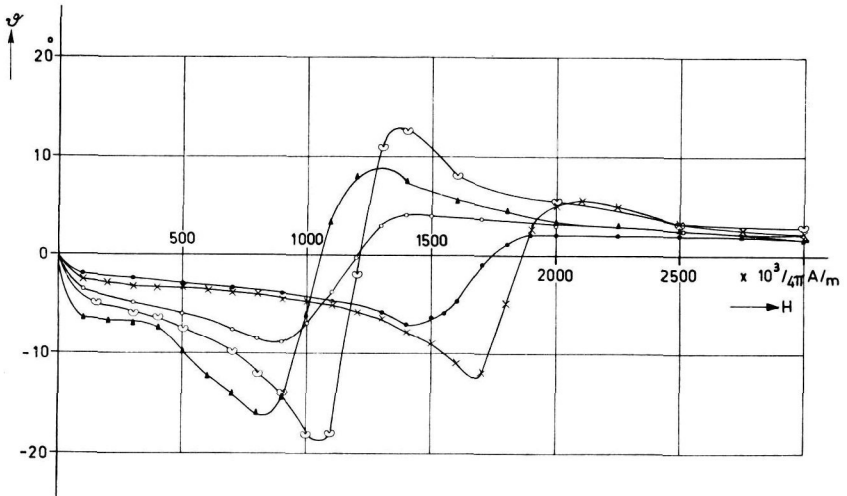


Fig. 8. Same as fig. 6, but for $\rho_1 = 0.1$ cm.

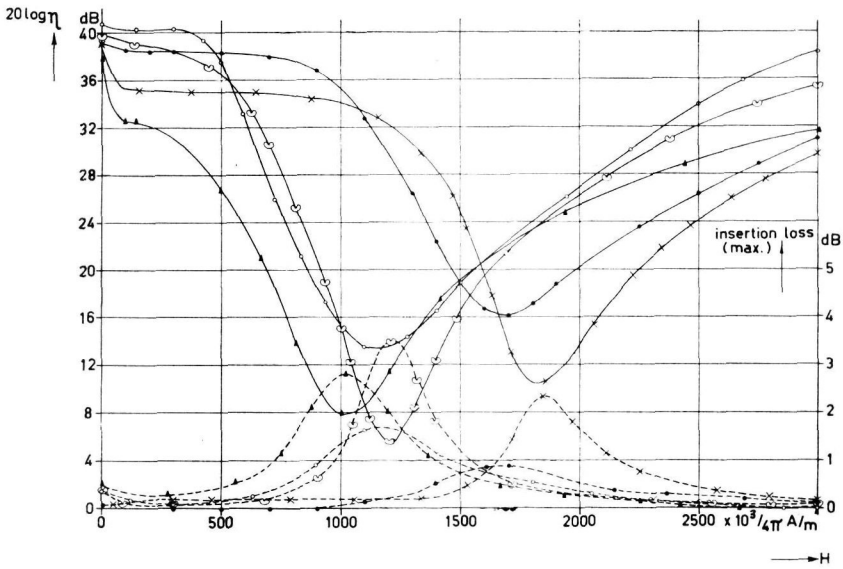


Fig. 9. Same as fig. 7, but for $\rho_1 = 0.1$ cm.

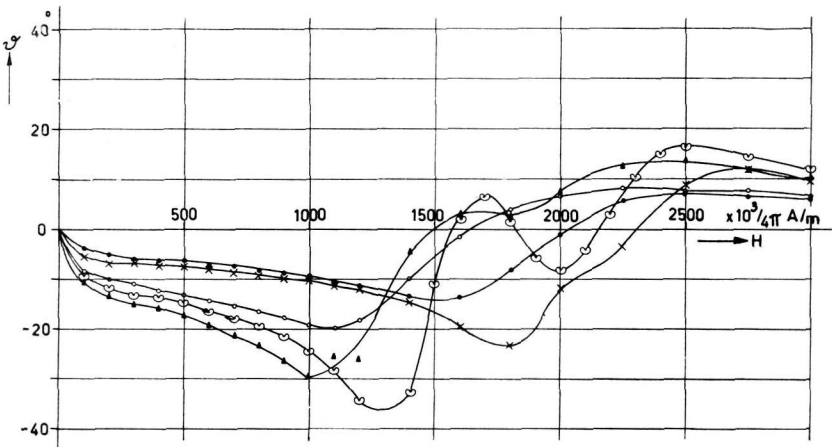


Fig. 10. Same as fig. 6, but for $\rho_1 = 0.15$ cm.

It appears from our measurements that H_r is a function of the radius ρ_1 of the rods. In figs 12, 13 and 14 H_r is shown for the different kinds of ferrite as a function of ρ_1 for $T = -32^\circ\text{C}$, room

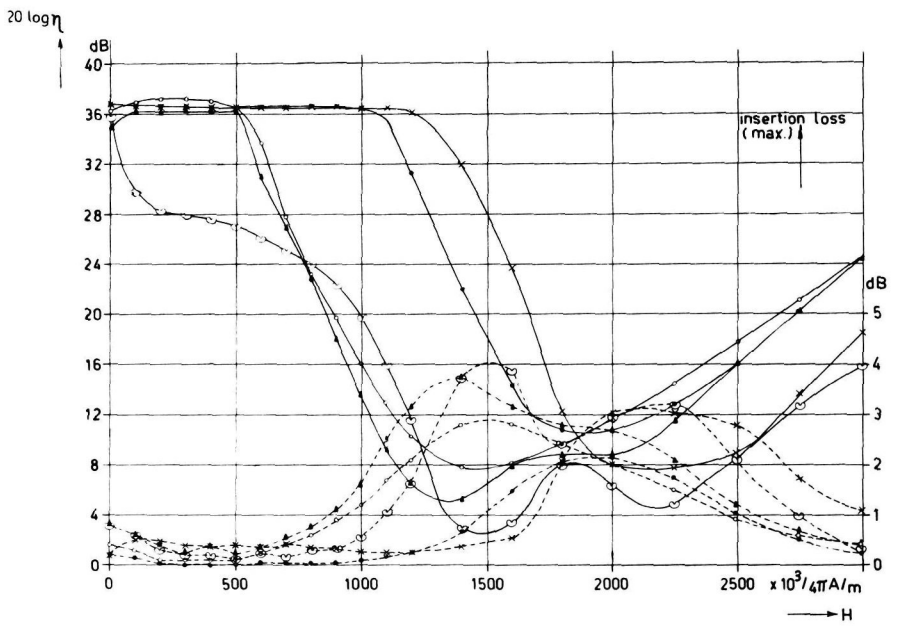


Fig. 11. Same as fig. 7, but for $\rho_1 = 0.15 \text{ cm}$.

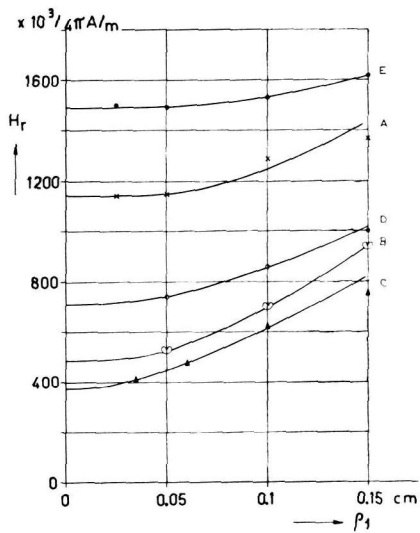
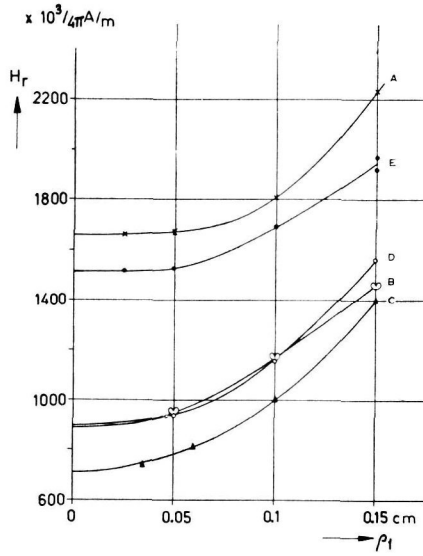
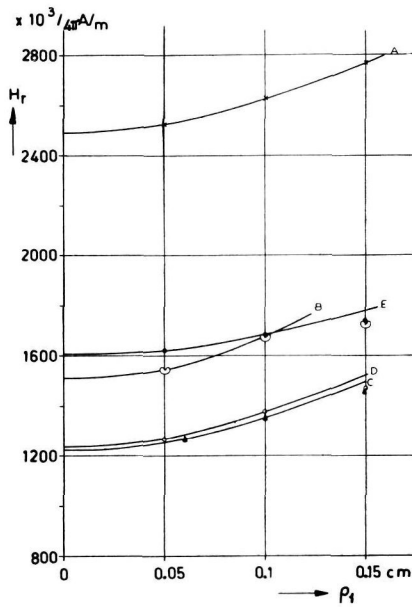


Fig. 12. The magnetic field strength at resonance H_r vs. the radius ρ_1 for rods of the ferrites A, B, C, D and E. $\lambda = 3.2 \text{ cm}$, $T = -32^\circ\text{C}$.

Fig. 13. Same as fig. 12, but for $T = 22^\circ\text{C}$.Fig. 14. Same as fig. 12, but for $T = 120^\circ\text{C}$.

temperature and 120°C . For some rods with a radius smaller than 0.5 mm no complete resonance curves have been obtained, but only the immediate neighbourhood of the resonance value H_r has been investigated in order to find H_r . These values of H_r have been included in figs 12, 13 and 14.

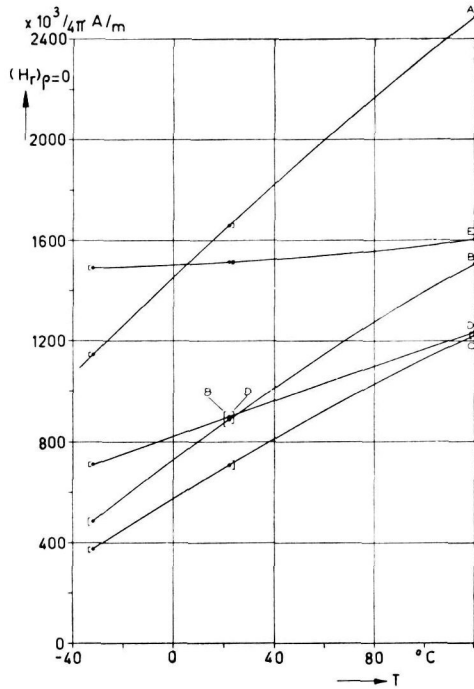


Fig. 15. The magnetic field strength at resonance H_r , extrapolated to vanishing radius ρ_1 of the ferrite rods, vs. the temperature. The brackets indicate the uncertainty of the extrapolation.

The phenomenological treatment of Chapter II is an approximation, valid only in the case of small radii ρ_1 . In order to be able in Chapter V et seq. to relate the atomistic theory of ferromagnetic resonance to our measurements we have extrapolated H_r in figs 12, 13 and 14 to $\rho_1 = 0$ and represented these extrapolated values of H_r as a function of the temperature in fig. 15.

§ 11. Sources of error in the rotation and ellipticity measurements. The phenomenological theory of Chapter II for the Faraday

rotation and ellipticity is based on the assumption that both the wave guide and the concentric rod are infinitely extended. The rods used by us were of finite length, and it is hence conceivable that end effects would introduce an error. It is to be expected that the relative size of this error will increase with increasing radius of the rods. Measurements of the Faraday rotation were therefore carried out for rods of the same radius and different lengths to see in how far the rotation angle was proportional to the length. For the rods ultimately used by us strict proportionality was found within the accuracy of the angular readings of about 0.1° if the radius did not exceed 1.5 mm. End corrections may then be neglected.

The error in the readings of the attenuator used to determine the ellipticity and insertion loss is about 0.1 db.

As can be seen from fig. 4, the static longitudinal magnetic field produced by the solenoid is not quite constant over the length $l = 3.45$ cm of the rods used. Since the rods were placed at the centre of the solenoid, the deviation from the average is about 1%.

The accuracy with which the temperature was defined was about 1°C . For this reason the data collected under the heading "room temperature" have been considered together, although actually this temperature lay between 20 and 22°C .

§ 12. *Measurements of the magnetization.* The magnetization for the various ferrite rods has been measured as a function of the magnetic field strength in the way described in § 7, for temperatures of -27° , 20° and 100°C . The results are given in fig. 16. The magnetization at saturation following from this figure is represented as a function of the temperature in fig. 17.

Some measurements of the initial permeability have also been made, the results being collected in table II.

TABLE II

$T = 20^\circ\text{C}$						
Ferrite	A'	A	B	C	D	E
Initial permeability	736	342	286	138	54.1	16.6

§ 13. *Resonance measurements on ferrite spheres.* Spheres of the ferrites mentioned in § 4, prepared in the way described there,

were studied for their behaviour in the presence of a static and a high frequency magnetic field by means of the apparatus discussed in § 9. At the wavelength $\lambda = 3.2$ cm a sphere of radius 0.2 mm, at $\lambda = 1.6$ cm and 1.25 cm a sphere of radius 0.125 mm was used.

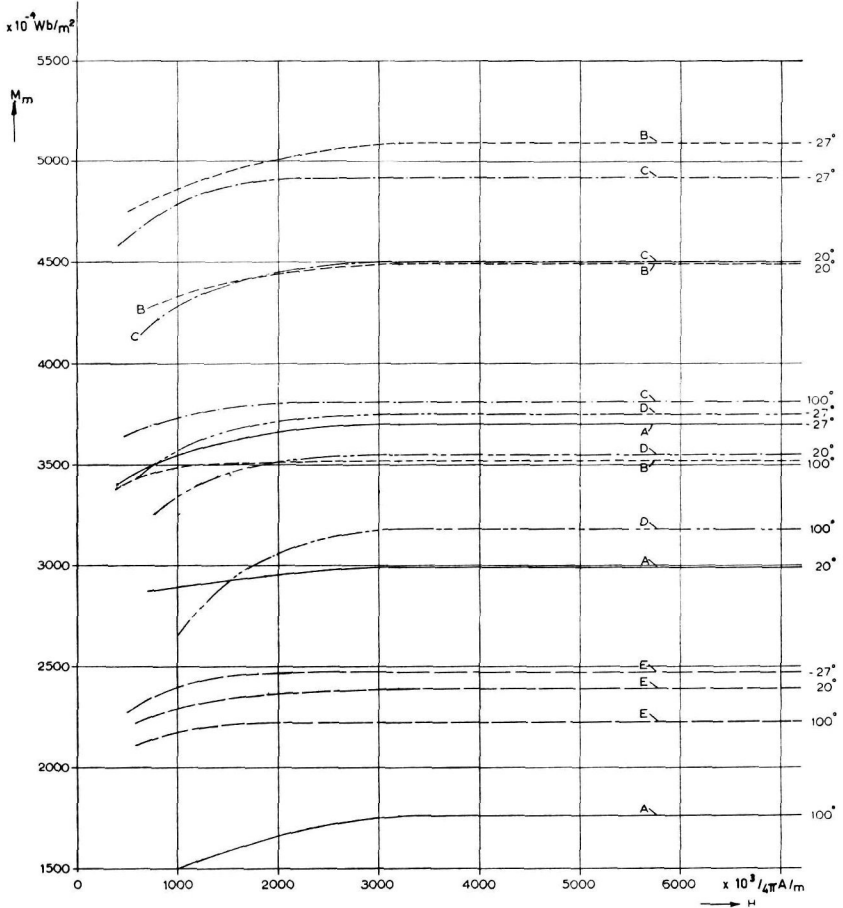


Fig. 16. The measured magnetization M_0 for the rods of ferrite A, B, C, D, E vs. the static magnetic field strength H_0 at temperatures $T = -27^\circ\text{C}$, $+20^\circ\text{C}$ and 100°C .

From the known angular frequency ω and the value H_r of the static magnetic field at which resonance occurred the gyromagnetic ratio Γ as defined by (3.1) could be determined.

In view of the theoretical discussion in the following chapters

we have expressed the Γ thus found in terms of the quantity $\mu_0 e/2m$ as unit, where e is the electronic charge and m the electronic mass:

$$\Gamma = g \frac{\mu_0 e}{2m}. \quad (4.1)$$

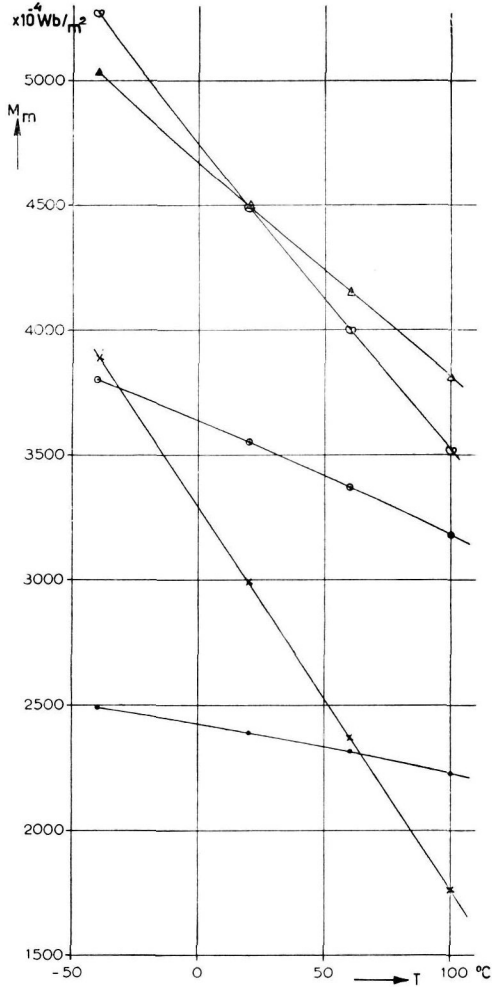


Fig. 17. The saturation magnetization for the ferrites A, B, C, D and E vs. the temperature.

For reasons that will become apparent later the quantity g , commonly called the spectroscopic splitting-factor, thus obtained is an effective one; we have denoted it by g_{eff} .

In figs 18–22 some of the results of our measurements with reference to g_{eff} have been represented graphically. Figs 18 and 19 show g_{eff} for the various ferrites as a function of the temperature T , the wavelength used being $\lambda = 3.2$ and 1.6 cm respectively. Figs 20, 21 and 22 show the dependence of g_{eff} on λ for the three temperatures $T = -30^\circ$, 20° and 100°C . This dependence has also been observed by Okamura and his collaborators ⁴).

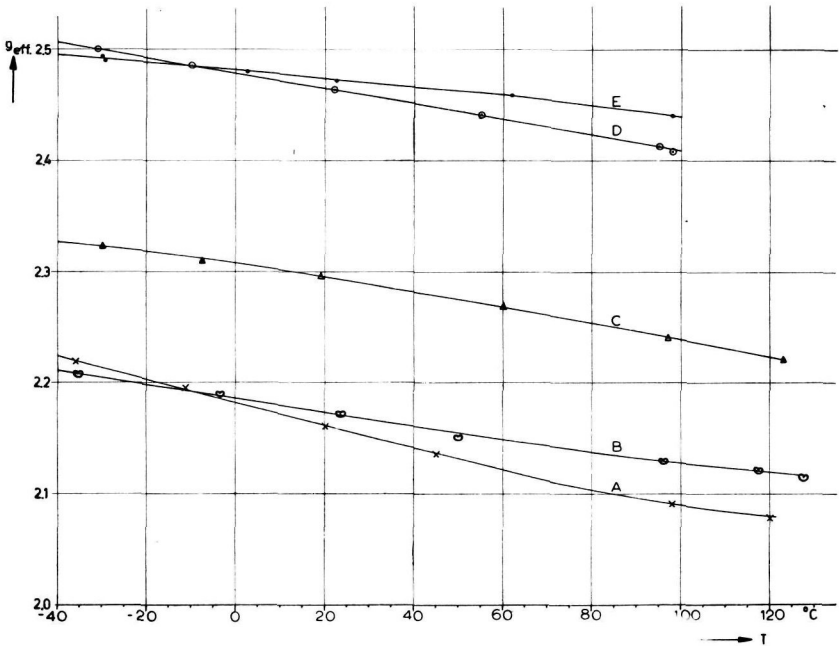


Fig. 18. The effective g -value for the ferrites A, B, C, D and E vs. the temperature at a wavelength $\lambda = 3.2$ cm, determined for spheres of radius 0.02 cm.

§ 14. *Sources of error in the resonance measurements.* In the resonance measurements on spheres reasonable care has to be taken to mount the spheres in the proper position on the axis inside the cavity. We have investigated how the value of g_{eff} , as defined in the preceding paragraph, is affected when the sphere is placed very close to the bottom of the cavity. Fig. 23 illustrates what happens for the case of a sphere of radius 0.125 mm. The explanation must be sought in the formation of images ⁵) ⁶). Reference ⁶) reports similar effects for a case of dielectric measurements.

Experimentally we also found that the value of g_{eff} depended somewhat on the diameter of the coupling holes both for reflection and transmission cavities. Fig. 24 illustrates this. The g -values obtained for different diameters of the coupling holes should

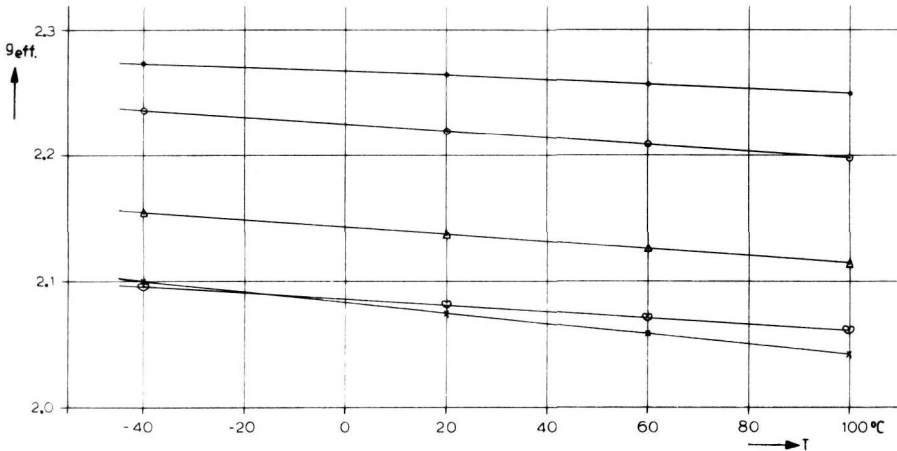


Fig. 19. The effective g -value for the ferrites A, B, C, D and E vs. the temperature at a wavelength $\lambda = 1.6$ cm for spheres of radius 0.0125 cm.

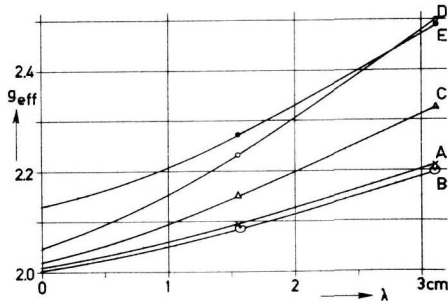


Fig. 20. The effective g -value for the ferrites A, B, C, D and E vs. the wavelength at a temperature $T = -30^\circ\text{C}$.

therefore be extrapolated to zero diameter for very accurate determinations.

On account of the small dimensions of the spheres the skin effect played no rôle in our measurements and the inaccuracy in

the values of the static magnetic field was less than in the rotation experiments, say 0.5%. The inaccuracy of the temperature T was the same in both cases, that is to say of the order of 1%. The values of g_{eff} are subject to an error of the same size.

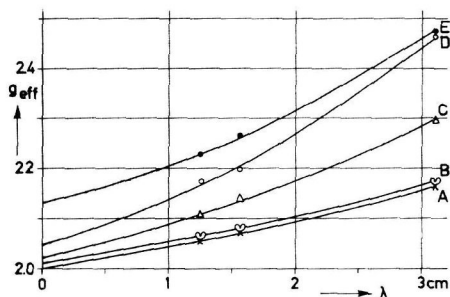


Fig. 21. Same as fig. 20, but for $T = 20^\circ\text{C}$.

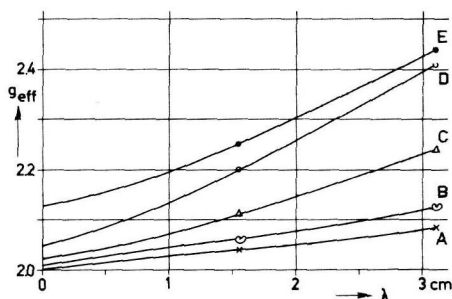


Fig. 22. Same as fig. 20, but for $T = 100^\circ\text{C}$.

It may be mentioned here that we checked our results for H_r with a Pound stabilized measuring equipment. Within an error of 0.5% agreement was found. With this apparatus the half-width ΔH_{oe} of the resonance curve (width at half the height of the maximum) could also be determined. The results are shown in table III. The measurements at $\lambda = 3.2$ cm were made on a sphere of 0.2 mm radius, those at $\lambda = 1.25$ cm on a sphere of 0.125 mm radius.

TABLE III

λ cm	3.2		1.25
T °C	- 40	20	20
Ferrite	ΔH_{oe} O	ΔH_{oe} O	ΔH_{oe} O
IV A	376	415	690
IV B	294	259	570
IV C	521	458	845
IV D	694	669	1265
IV E	910	856	

CHAPTER V. INTERPRETATION OF THE ROTATION AND ELLIPTICITY MEASUREMENTS IN TERMS OF FERROMAGNETIC RESONANCE

§ 15. *The permeability tensor.* The theory of ferromagnetic resonance starts from the fundamental equation, first given by

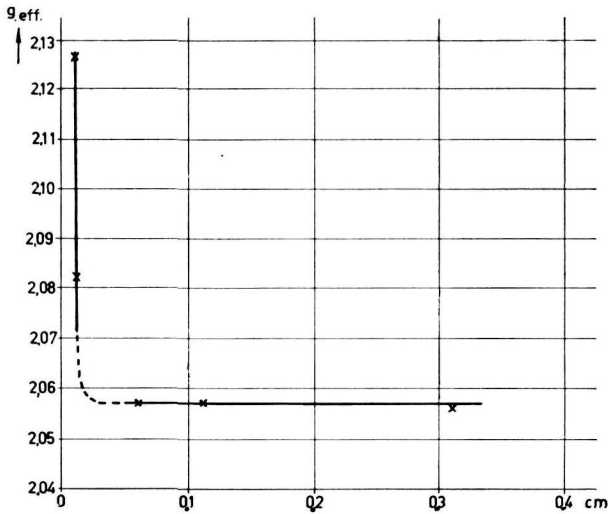


Fig. 23. The effective g -value for a sphere of ferrite A of radius 0.0125 cm at a temperature $T = 20^\circ\text{C}$ and a wavelength $\lambda = 1.25$ cm as a function of the distance between the centre of the sphere and the wall: "Wall effect".

Landau and Lifschitz ⁷⁾, for the time dependence of the magnetization \mathbf{M}

$$\frac{d\mathbf{M}}{dt} = \Gamma \mathbf{M} \times \mathbf{H} - \frac{\kappa \Gamma}{M} \mathbf{M} \times (\mathbf{M} \times \mathbf{H}), \quad (5.1)$$

where Γ is the gyromagnetic ratio, already referred to in § 13, \mathbf{H}

the local magnetic field strength acting on the magnetization and κ a damping constant. Without the damping term (5.1) formed the basis of the original considerations of Kittel⁸⁾.

In the thesis of van Trier¹⁾ previously mentioned expressions for the elements of the gyromagnetic permeability tensor (2.1) have

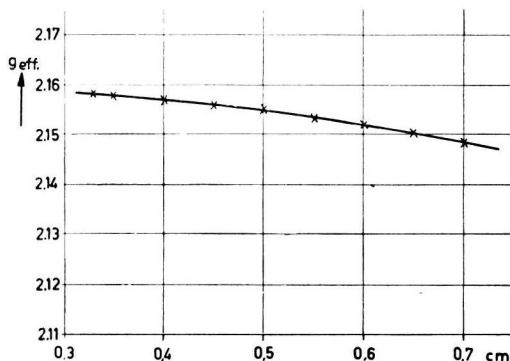


Fig. 24. The effective g -value for a sphere of ferrite A of radius 0.02 cm at a temperature $T = 20^\circ\text{C}$ and a wavelength $\lambda = 3.2$ cm as a function of the radius of the coupling hole in the resonance cavity.

been derived from (5.1) for the case of no losses $\kappa = 0$. The procedure followed by him can be generalized to the case $\kappa \neq 0$.

If in a given region of the ferromagnetic medium we choose a local coordinate system such that its z -axis, carrying the unit vector \mathbf{k} , coincides with the static part of the magnetic field $H_0\mathbf{k}$ there, then the magnetic field may be written as

$$\mathbf{H} = H_0\mathbf{k} + \mathbf{H}_1 \exp j\omega t, \quad (5.2)$$

the second term on the right-hand side being the high frequency part of the magnetic field. Similarly we may split the magnetization into its static and high frequency parts:

$$\mathbf{M} = M_0\mathbf{k} + \mathbf{M}_1 \exp j\omega t. \quad (5.3)$$

On the assumption, always realized in our experiments, that $H_1 \ll H_0$, $M_1 \ll M_0$ we may on substitution of (5.2) and (5.3) in (5.1) neglect terms of second and third degree in quantities bearing the index 1 and get thus

$$j\omega\mathbf{M}_1 = \Gamma(H_0\mathbf{M}_1 - M_0\mathbf{H}_1) \times \mathbf{k} + \kappa \Gamma[(H_0\mathbf{M}_1 - M_0\mathbf{H}_1) \times \mathbf{k}] \times \mathbf{k}. \quad (5.4)$$

Writing the high frequency part of the magnetic induction with the aid of the gyromagnetic permeability tensor (2.1), (2.2) as

$$\mathbf{B}_1 = \mu_0 \mathbf{H}_1 + \mathbf{M}_1 = \|\mu\| \mathbf{H}_1$$

or in components

$$\left. \begin{aligned} B_{1x} &= \mu_0 H_{1x} + M_{1x} = (\mu_1' - j\mu_1'') H_{1x} - j(\mu_2' - j\mu_2'') H_{1y}, \\ B_{1y} &= \mu_0 H_{1y} + M_{1y} = j(\mu_2' - j\mu_2'') H_{1x} + (\mu_1' - j\mu_1'') H_{1y}, \\ B_{1z} &= \mu_0 H_{1z} + M_{1z} = (\mu_3' - j\mu_3'') H_{1z}, \end{aligned} \right\} (5.5)$$

we find by solving (5.4) for the components of \mathbf{M}_1 , substituting into (5.5) and equating the coefficients of H_{1x} and H_{1y} on the right and left

$$\mu_1' = \mu_0 + \frac{\Gamma^2 M_0 H_0 \{ (1 + \kappa^2) [(1 + \kappa^2) \Gamma^2 H_0^2 - \omega^2] + 2\kappa^2 \omega^2 \}}{[(1 + \kappa^2) \Gamma^2 H_0^2 - \omega^2]^2 + 4\kappa^2 \omega^2 \Gamma^2 H_0^2}, \quad (5.6)$$

$$\mu_1'' = \frac{\kappa \omega \Gamma M_0 [(1 + \kappa^2) \Gamma^2 H_0^2 + \omega^2]}{[(1 + \kappa^2) \Gamma^2 H_0^2 - \omega^2]^2 + 4\kappa^2 \omega^2 \Gamma^2 H_0^2}, \quad (5.7)$$

$$\mu_2' = \frac{\omega \Gamma M_0 [(1 + \kappa^2) \Gamma^2 H_0^2 - \omega^2]}{[(1 + \kappa^2) \Gamma^2 H_0^2 - \omega^2]^2 + 4\kappa^2 \omega^2 \Gamma^2 H_0^2}, \quad (5.8)$$

$$\mu_2'' = \frac{2\kappa \omega^2 \Gamma^2 M_0 H_0}{[(1 + \kappa^2) \Gamma^2 H_0^2 - \omega^2]^2 + 4\kappa^2 \omega^2 \Gamma^2 H_0^2}. \quad (5.9)$$

The quantities (5.6)–(5.9) may be termed the local values of the elements of the permeability tensor since they refer to the local coordinate system introduced. Let us now suppose

a) that the ferromagnetic medium is subjected to a homogeneous external static field \mathbf{H}_{0e} of such magnitude as to give rise to magnetic saturation,

b) that the specimen used is of ellipsoidal shape and that in consequence the demagnetizing static field is also homogeneous,

c) that the fields due to crystal anisotropy and magnetostriction are negligible,

then both \mathbf{H}_0 and \mathbf{M}_0 will have the same magnitude and direction everywhere in the specimen and the expressions (5.6)–(5.9) may be regarded as the elements of the permeability tensor with respect to one and the same coordinate system with the z -axis in the direction of \mathbf{H}_0 at all points of the medium.

Both in our experiments on the Faraday rotation in rods and on ferromagnetic resonance in spheres the fields in the resonance region, of the order 1000–8000 oerstedt, were such that magnetic saturation was at least approximately realized, as can be seen by inspection of fig. 16. Also the rods used were so thin compared with their length that they may be identified with the limiting case of a very elongated ellipsoid for which the internal static field H_0 is practically equal to the external static field H_{0e} applied in a longitudinal direction, the demagnetizing field practically vanishing. Finally the anisotropy fields may indeed, at the field strengths of interest, be considered as small corrections.

A feature which we shall forget at present is the fact that the materials investigated, due to their porosity, actually are not homogeneous. The influence of the porosity will form the subject of the following chapters.

§ 16. *Ferromagnetic resonance in spheres.* Inside a sphere placed in a homogeneous external magnetic field the resultant magnetic field is equal to the external field diminished by one third of the magnetization divided by μ_0 . Thus if the sphere is small compared with the wavelength of the high frequency field we have both

$$H_0 = H_{0e} - M_0/3\mu_0, \quad H_1 = H_{1e} - M_1/3\mu_0.$$

Let us take \mathbf{H}_{0e} in the z -direction, \mathbf{H}_{1e} in the x -direction. Then we find from (5.4)

$$\begin{aligned} j\omega M_{1x} &= \Gamma H_{0e} M_{1y} - \kappa \Gamma H_{0e} M_{1x} + \kappa \Gamma M_0 H_{1e}, \\ j\omega M_{1y} &= -\Gamma H_{0e} M_{1x} + \Gamma M_0 H_{1e} - \kappa \Gamma H_{0e} M_{1y}. \end{aligned}$$

Solving for M_{1x} and M_{1y} from these two equations, expressions are obtained with the denominator

$$[(1 + \kappa^2) \Gamma^2 H_{0e}^2 - \omega^2]^2 + 4\kappa^2 \omega^2 \Gamma^2 H_{0e}^2,$$

showing that resonance occurs for a value H_r of H_{0e} given by

$$\omega = \Gamma H_r \sqrt{1 + \kappa^2}. \quad (5.10)$$

Since we shall find later that κ in the ferrites studied averages about 0.05 and is never more than 0.1, we see that the damping correction influences (5.10) at most by $\frac{1}{2}\%$ and may hence be neglected in view of the accuracy of our measurements. The experimental definition of Γ as given in (3.1) is thereby justified.

§ 17. *Determination of the damping constant κ from the rotation and ellipticity measurements.* We proceed now to compute numerically from (5.6)–(5.9) the quantities μ_1' , μ_1'' , μ_2' , μ_2'' for the frequency

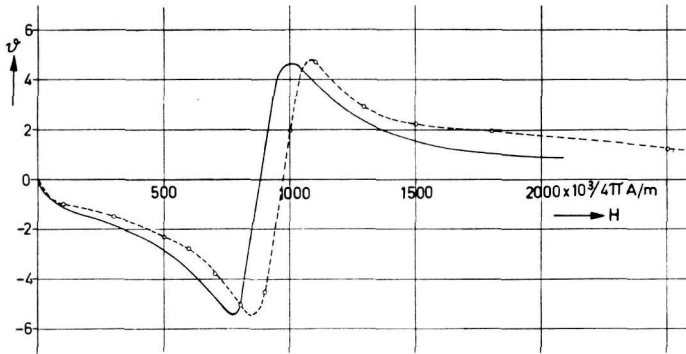


Fig. 25. Measured (---) and calculated (—) rotation angle θ as a function of the static magnetic field strength for a rod of ferrite B of length $l = 3.5$ cm and radius $\rho_1 = 0.05$ cm at a wavelength $\lambda = 3.2$ cm and a temperature $T = 20^\circ\text{C}$. In the calculation the following values were used $\kappa = 0.032$, $g_{\text{eff}} = 2.12$, $M_0 = 0.456$ Wb/m².

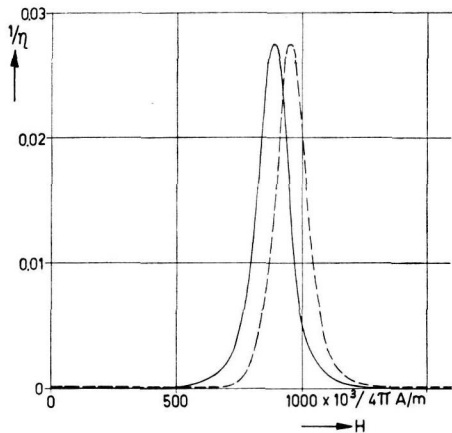


Fig. 26. Measured (---) and calculated (—) reciprocal ellipticity $1/\eta$ for the case of fig. 25.

9375 MHz, corresponding to the wavelength $\lambda = 3.2$ cm used in the Faraday rotation experiments, for various temperatures and for various values of the external field, which, as previously mentioned, may here be identified with the quantity H_0 in the above equations.

For I we employ the value of the gyromagnetic ratio found from measurements of the resonance field H_r in a sphere of the same material and at the same frequency and temperature, as described in § 13. For M_0 we introduce the value of the magnetization at the temperature and magnetic field strength under consideration. Finally we assume a tentative value for κ .

The values of μ_1' , μ_1'' , μ_2' , μ_2'' thus obtained are then substi-

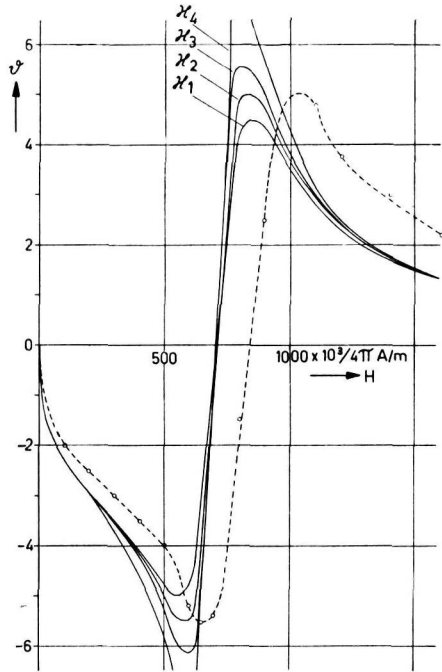


Fig. 27. Influence of the choice of κ on the calculated rotation angle ϑ for a rod of ferrite C of length $l = 3.5$ cm and radius $\rho_1 = 0.06$ cm at a wavelength $\lambda = 3.2$ cm and a temperature $T = 20^\circ\text{C}$. In the calculation the following values were used $\kappa_1 = 0.05$, $\kappa_2 = 0.045$, $\kappa_3 = 0.04$, $\kappa_4 = 0.03$, $g_{\text{eff}} = 2.244$, $M_0 = 0.456$ Wb/m².

tuted in the expressions (2.8) en (2.9) for the quantities α_{\pm} and β_{\pm} , which in their turn determine the value of the rotation angle ϑ and the ellipticity η according to (2.12) and (2.14).

Figs 25 and 26 show for a rod of ferroxcube IV B both the measured curves for ϑ and $1/\eta$ and the curves calculated in the way just described, using the value $\kappa = 0.032$ which gave the best fit.

It is seen that the theoretical and experimental curves agree very well except that the theoretical curves at resonance are shifted over a distance of about 70 oersted to the left with respect to the experimental curves. This can be understood if it is remembered that (2.8) and (2.9) hold strictly only in the limit of vanishing radius of the rod. Indeed, experiments with rods of different radii show that

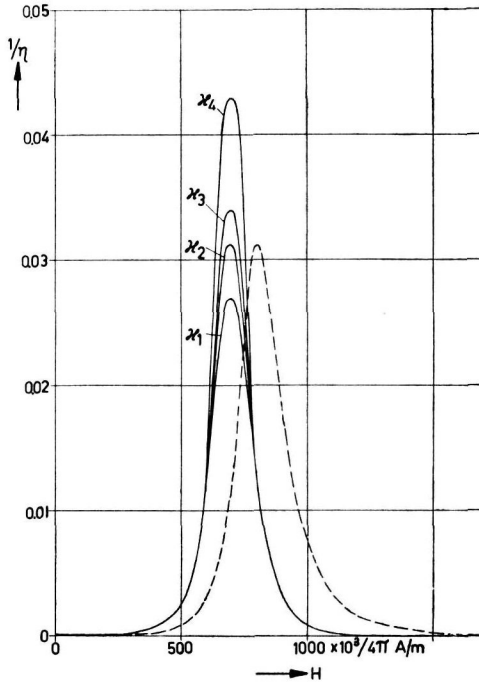


Fig. 28. Influence of the choice of κ on the calculated ellipticity, same case as fig. 27.

the shift decreases toward zero with diminishing radius. Also it is found that κ is practically unaffected by variations in ρ_1 .

An impression of the sensitivity of the computed curves for the choice of κ is given by figs 27 and 28 which refer to rotation and ellipticity measurements in ferroxcube IV C. Here too the shift already mentioned manifests itself. It is clear that the value $\kappa_2 = 0.045$ gives the best fit and that the adjustment is rather critical.

Figs 29 and 30 represent the values of κ thus obtained for the

different ferrites as a function of the temperature and the porosity respectively. Fig. 31 shows that there is no very simple connection between κ and the percentage NiO contained in the ferrites. To the interpretation of these results we shall return in Chapter VII.

It is interesting to compute the resonance value H_r of the field at which the rotation angle ϑ vanishes. According to (2.12) this requires $\beta_+ - \beta_- = 0$. Using (2.9) we thus find the condition

$$[(\mu_1' + \mu_0)^2 - \mu_2'^2 - \mu_1''^2 - \mu_2''^2] \mu_2' + 2(\mu_1' + \mu_0) \mu_1'' \mu_2'' = 0. \quad (5.11)$$

With the expressions (5.6) to (5.9) for μ_1' , μ_1'' , μ_2' , μ_2'' it is verified by substitution that (5.11) is satisfied if we put for H_0 the value

$$H_r = \frac{\omega}{\Gamma \sqrt{1 + \kappa^2}} - \frac{M_0}{2\mu_0}. \quad (5.12)$$

TABLE IV

T °C	ferrite	$(H_r)_{exp}$ O	$(H_r)_{calc}$ M_0 at H_r O	$(H_r)_{calc}$ M_0 at saturation O
- 27	A	1190 ± 9	1228 ± 24	1166 ± 24
	B	525 ± 17	652 ± 28	484 ± 28
	C	405 ± 13	539 ± 27	371 ± 27
	D	728 ± 13	910 ± 22	880 ± 22
	E	1490 ± 14	1438 ± 20	1428 ± 20
20	A	1639 ± 10	1617 ± 22	1589 ± 22
	B	874 ± 33	916 ± 26	824 ± 26
	C	695 ± 17	913 ± 26	648 ± 26
	D	890 ± 24	1021 ± 23	899 ± 23
	E	1510 ± 10	1503 ± 20	1478 ± 20
100	A	2331 ± 16	2344 ± 20	2317 ± 20
	B	1391 ± 27	1384 ± 25	1377 ± 25
	C	1123 ± 18	1202 ± 25	1072 ± 25
	D	1168 ± 19	1366 ± 22	1161 ± 22
	E	1580 ± 17	1608 ± 20	1603 ± 20

The third column in table IV gives the experimental values of H_r in oerstedt, extrapolated to zero value of the radius ρ_1 of the ferrite rods as shown in figs 12, 13, 14 and 15, the fourth column the values calculated from (5.12). In the majority of cases the experimental values are equal, within the experimental error, to the theoretical ones or somewhat lower, the difference increasing with decreasing H_r . This can be understood if we remember that at the

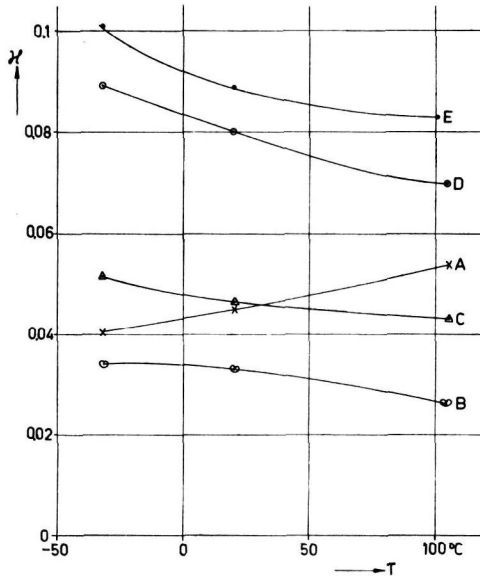


Fig. 29. The damping constant κ for the ferrites A, B, C, D, E as a function of the temperature.

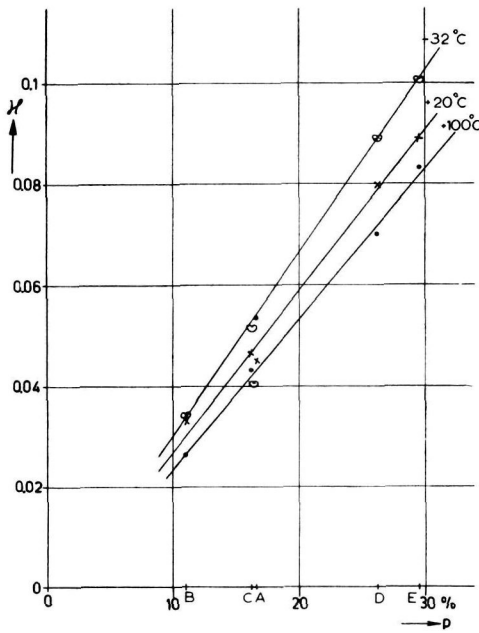


Fig. 30. The damping constant κ for the ferrites A, B, C, D, E as a function of the porosity for the temperatures $T = -32^\circ\text{C}$, 20°C and 100°C .

lower field strengths we have not yet attained full magnetic saturation (see fig. 16). As we have mentioned before, our theoretical expressions in the first place hold strictly only when saturation is attained. But besides, as we shall see in the following chapter, the porosity actually makes the magnetic field inhomogeneous in the

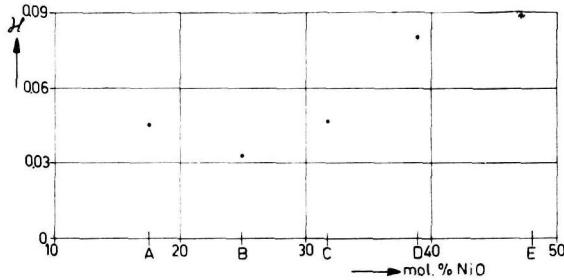


Fig. 31. The damping constant κ for the ferrites A, B, C, D, E as a function of the percentage NiO at a temperature $T = 20^\circ\text{C}$.

material and lets the field strength take on local values greater than the average. The values of M_0 which ought to be substituted in our equations are hence larger than those corresponding to the external static field H_0 . By using for M_0 the magnetization at saturation, we should get a lower bound for H_r as computed from theory. In the fifth column of table IV these values have also been given.

CHAPTER VI. THE INFLUENCE OF POROSITY ON THE RESONANCE CONDITIONS

§ 18. *Outline of the problem.* In view of the available measuring equipment and because of its simplicity we have studied the resonance phenomenon in spheres of ferrite over a wider range of conditions than the Faraday rotation in rods. For a sphere we found in § 15 the resonance relation (5.10), which on account of the small value of κ (< 0.1) practically reduces to the relation (3.1). As mentioned already in § 13 it is customary for purposes of theory to express Γ in the unit $\mu_0 e / 2m$ by means of (4.1), leading us to the spectroscopic splitting factor g .

If the magnetization of a substance is entirely due to electron spins, one expects the value $g = 2$. As discussed e.g. by Van Vleck⁹⁾,

g may become larger, say $2 + \delta$, if the electronic orbital motion also contributes to the magnetization. In most ferromagnetics δ lies below 0.1. Besides g another quantity g' , the magneto-mechanical factor plays a rôle in magnetized media. It represents the ratio of the magnetic moment to the mechanical moment of momentum manifesting itself in the Einstein-de Haas effect, again expressing this ratio in the unit $\mu_0 e / 2m$. For small values of δ theory^{10) 11)} shows that $g' = 2 - \delta$, so that we have the relation $g - 2 = 2 - g'$. In conformity with this relation also g' in general is found to differ from 2 by less than 0.1. By reason of its fundamental physical significance g should be essentially a constant characteristic of the material and hence independent of the wavelength used in the resonance experiments and of the temperature.

In contrast to other ferromagnetics our figs 18 to 22 show effective g -values ranging up to 2.5. In addition the values g_{eff} are seen to depend noticeably on the temperature and strongly on the wavelength employed. It is the purpose of this chapter to investigate the causes of these discrepancies.

The dependence of g_{eff} on wavelength had already been noted by Okamura and his collaborators^{4) 12)}. This author introduced into the resonance equation an internal field H_i , which he assumed to be temperature-dependent, by writing instead of (3.1)

$$\omega = \Gamma(H_r + H_i).$$

By measuring H_r at two different frequencies, Γ and H_i could then be computed. Suggestions were made about the physical origin of the field H_i without leading to definite conclusions.

§ 19. *The influence of porosity on the g -values.* Polycrystalline ferrites are sintered materials always showing pores. It is impossible to prepare them with the same bulk behaviour, but without porosity. Having arisen in a partially melted material of a ceramic nature, the pores may reasonably be assumed to have in general a spherical shape due to the effects of surface tension, a hypothesis confirmed by microphotographs of polished sections. A polycrystalline ferrite may hence be considered as pure ferrite with inclusions of air.

In this section we shall proceed as if the ferrites used in our experiments were homogeneous substances for which the magnetization due to a given static external field H_{0e} , and hence also the

demagnetizing field, has a value differing from that in an ideal ferrite without air inclusions. We shall then calculate the external field $H_{0e'}$ that would have to be applied to the ideal ferrite in order to make the internal field the same as in the real ferrite.

For a homogeneous sphere of the real ferrite the external field H_{0e} , the internal field H_0 and the magnetization M_0 are related by

$$H_{0e} = H_0 + \frac{M_0}{3\mu_0}. \quad (6.1)$$

For the ideal ferrite at the same internal field H_0 we have similarly

$$H_{0e'} = H_0 + \frac{M_0'}{3\mu_0}. \quad (6.2)$$

Hence from (6.1) and (6.2)

$$H_{0e'} = H_{0e} + H_p, \quad (6.3)$$

the corrective field H_p due to porosity being

$$H_p = \frac{M_0' - M_0}{3\mu_0}. \quad (6.4)$$

Since the magnetization M_0 in the real ferrite, on account of the presence of air, will be less at the same internal field strength H_0 than the magnetization M_0' of the ideal ferrite, H_p is positive. If we could have performed our resonance experiments on a sphere of the ideal ferrite, we would have found a larger resonance field strength H_r' for a given frequency ω and accordingly from (3.1) and (4.1) a smaller g -value provided the effect of the pores on the high frequency field can be neglected.

There are two cases for which the difference $M_0' - M_0$ in (6.4) can be calculated exactly. The simplest is the one where the magnetization may be assumed to have everywhere the same fixed value M_0 in the direction of the external field, irrespective of whether the sphere be solid or porous, so that on removing the ferromagnetic material from the solid sphere in the regions occupied by the pores, the magnetization remains "frozen in" in the rest of the material both as regards magnitude and direction. Then evidently the magnetization M_0 of the real ferrite is $(1 - q)$ times the magnetization M_0' of the ideal ferrite, q being the fraction of the volume occupied by the pores. Hence

$$M_0' = \frac{1}{1 - q} M_0, \quad M_0' - M_0 = \frac{q}{1 - q} M_0 \quad (6.5)$$

and from (6.4)

$$H_p = \frac{p}{100 - p} \frac{M_0}{3\mu_0} \quad (6.6)$$

if we express the porosity $p = 100q$ in per cent. Clearly this expression is a lower bound, for even at saturation the introduction of the pores will disorientate the magnetization and thereby increase $M_0' - M_0$ above the value (6.5).

The second case amenable to exact treatment is that of a linear medium in which the magnetization is everywhere proportional to the local magnetic field strength and parallel to it. Then the law of mixtures due to Maxwell¹³⁾ can be applied, leading to

$$\frac{M_0' - M_0}{3\mu_0 H_0 + M_0 + 2M_0'} = q \frac{M_0'}{3\mu_0 H_0 + 2M_0'}, \quad (6.7)$$

M_0 and M_0' being the values of the magnetization at the same internal field strength H_0 for the real and the ideal ferrite. Now the external field strength H_{0e} for a sphere of the real ferrite is related to H_0 by (6.1). Introducing H_{0e} instead of H_0 in (6.7) this becomes

$$\frac{M_0' - M_0}{3\mu_0 H_{0e} + 2M_0'} = q \frac{M_0'}{3\mu_0 H_{0e} - M_0 + 2M_0'}. \quad (6.8)$$

For the quantity $\Delta M_0 = M_0' - M_0$ we get from (6.8) the quadratic equation

$$2(1 - q)(\Delta M_0)^2 + [(1 - q)3\mu_0 H_{0e} + (1 - 4q)M_0] \Delta M_0 - q(3\mu_0 H_{0e} + 2M_0)M_0 = 0.$$

Its positive solution, expanded in powers of q up to the second power is

$$M_0' - M_0 = \frac{q}{1 - q} \frac{(3\mu_0 H_{0e} + 2M_0)M_0}{3\mu_0 H_{0e} + M_0} \left[1 + q \frac{(3\mu_0 H_{0e} - M_0)M_0}{(3\mu_0 H_{0e} + M_0)^2} + \dots \right]. \quad (6.9)$$

Using again $p = 100q$ to describe the porosity in per cent, we have from (6.4) and (6.9)

$$H_p = \frac{p}{100 - p} \frac{(3\mu_0 H_{0e} + 2M_0)M_0}{3\mu_0(3\mu_0 H_{0e} + M_0)} \cdot \left[1 + \frac{p}{100} \frac{(3\mu_0 H_{0e} - M_0)M_0}{(3\mu_0 H_{0e} + M_0)^2} + \dots \right]. \quad (6.10)$$

For the high field strengths $H_{0e} = H_r$ of more than 2500 O at which in our experiments resonance occurs the real ferrite may be expected to behave in good approximation according to (6.10). The magnetization, it is true, does not vary linearly with H_0 , being near saturation, but the effective susceptibility M_0/H_0 changes only slightly in the small range of values taken by the local field in the neighbourhood of the pores. The direction of the magnetization on the other hand, will everywhere be parallel to that of the local field, as assumed in the derivation.

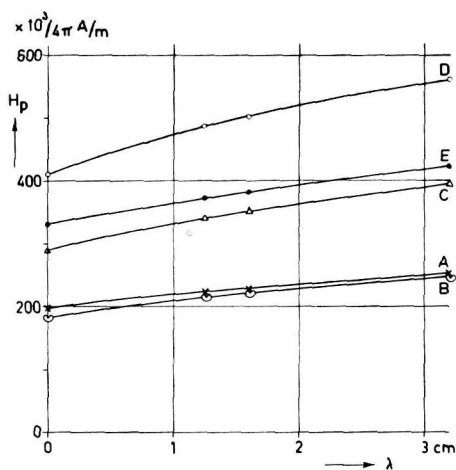


Fig. 32. The corrective field H_p according to (6.10) vs. the wavelength at a temperature $T = 20^\circ\text{C}$.

In fig. 32 we have represented the field H_p as given by (6.10) for the various ferrites at resonance as a function of the wavelength λ , the temperature being $T = 20^\circ\text{C}$. As λ goes to zero, the value of the external field H_{0e} at which resonance occurs increases indefinitely. Since M_0 does not exceed its saturation value, it then follows from (6.10) that H_p for $\lambda \rightarrow 0$ approaches the value (6.6) as a limit. In fig. 32 this value is hence represented by the intercept of the curves with the ordinate axis. The figure shows that the amount by which H_p exceeds this lower bound in general is less than 30 per cent at the wavelengths considered. In figs 33 and 34 the field H_p following from (6.10) is shown for the various ferrites as a function of the temperature T , fig. 33 referring to resonance at $\lambda = 3.2 \text{ cm}$, fig. 34

to resonance at $\lambda = 1.6$ cm. The order of magnitude of H_p runs from about 100 to 600 oersted.

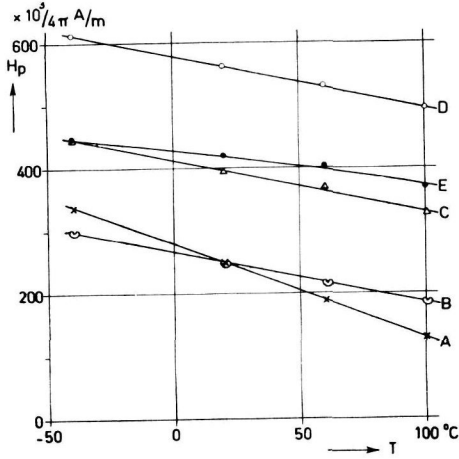


Fig. 33. The corrective field H_p according to (6.10) vs the temperature for a wavelength $\lambda = 3.2$ cm.

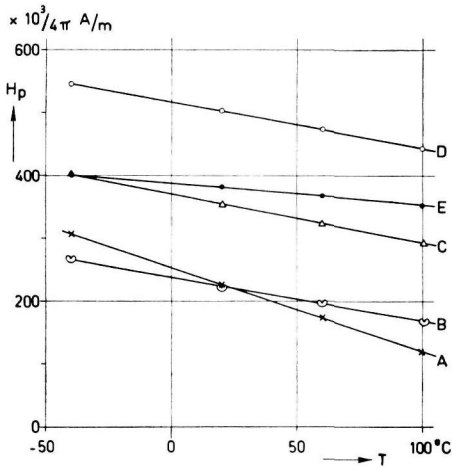


Fig. 34. Same as fig. 33, but for $\lambda = 1.6$ cm.

With the values of H_p given by (6.10) new g -values g_p have been computed by writing

$$\omega = \Gamma(H_r + H_p). \quad (6.11)$$

These g_p values are shown in tables V and VI. It is seen that the

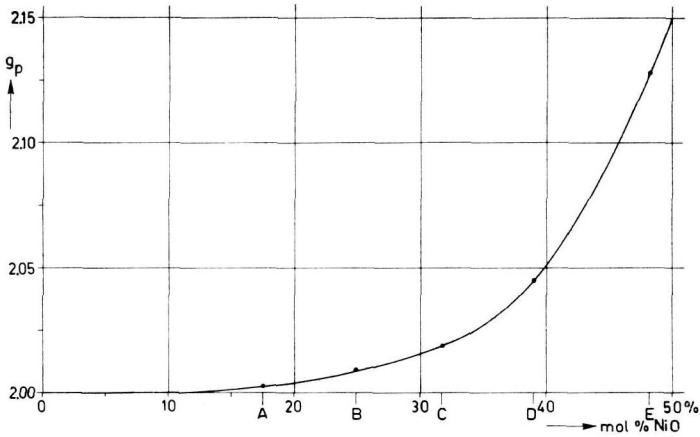
Fig. 35. The g -value corrected for porosity vs. the percentage NiO.

TABLE V

Ferrite	T °C	$\lambda = 3.2$ cm				$\lambda = 1.6$ cm			
		H_r O	$M_0 \mu_0$ O	H_p O	g_p	H_r O	$M_0 \mu_0$ O	H_p O	g_p
IV A	— 40	2993	3890	340	2.00	6320	3890	308	2.00
	20	3078	2990	252	2.00	6397	2990	229	2.00
	60	3138	2370	193	2.00	6447	2370	177	2.00
	100	3190	1660	129	2.01	6497	1660	120	2.01
IV B	— 40	3012	5270	300	2.01	6330	5270	268	2.01
	20	3064	4490	248	2.01	6378	4490	222	2.01
	60	3099	4000	217	2.01	6407	4000	195	2.01
	100	3130	3520	187	2.01	6437	3520	167	2.01
IV C	— 40	2861	5030	449	2.01	6156	5030	401	2.02
	20	2900	4500	396	2.02	6208	4500	353	2.02
	60	2935	4150	371	2.01	6241	4150	322	2.02
	100	2974	3810	325	2.02	6277	3810	292	2.02
IV D	— 40	2652	3800	613	2.04	5933	3800	544	2.05
	20	2700	3550	564	2.04	5977	3550	503	2.05
	60	2733	3370	532	2.04	6007	3370	474	2.05
	100	2766	3185	496	2.04	6038	3185	445	2.05
IV E	— 40	2668	2490	445	2.14	5837	2490	401	2.13
	20	2691	2390	425	2.14	5860	2390	382	2.13
	60	2709	2310	407	2.14	5877	2310	369	2.12
	100	2729	2225	390	2.13	5895	2225	354	2.12

TABLE VI

Ferrite	T °C	$\lambda = 1.25$ cm			
		H_r O	$M_0 \mu_0$ O	H_p O	g_p
IV A	20	8331	2990	224	2.00
IV B		8316	4490	216	2.01
IV C		8144	4500	340	2.02
IV D		7887	3550	486	2.05
IV E		7704	2390	372	2.12

values of g_p lie much closer to 2 than the values g_{eff} shown in figs 18 — 22 and moreover are independent of T and λ . In fig. 35 g_p is shown as a function of the percentage NiO.

CHAPTER VII. THE INFLUENCE OF POROSITY ON THE LINE WIDTH

§ 20. *Outline of the problem.* Consider a sphere of ideal non-porous ferrite placed in a homogeneous external static magnetic field of sufficient strength to produce approximately saturation. The field inside the sphere will then be homogeneous. A cavity, introduced into the ferrite, will give rise in its neighbourhood to a distortion of the internal field, both as regards magnitude and direction. On applying an alternating magnetic field of given angular frequency, the different volume elements of the ferrite around the cavity will hence be in resonance at different values of the external field. The resonance absorption, when represented as a function of the external field will consequently show a broadening, suitably termed porosity broadening.

In the next paragraph we shall try to arrive at a rough estimate of this broadening under the following simplifying assumptions.

a) The ferrite is supposed to behave as a linear medium in the sense discussed in § 19, meaning that the magnetization is everywhere parallel and proportional to the local field. In § 19 we saw that at the high field strengths necessary for resonance in our experiments on ferrites this assumption is reasonably close to reality.

b) The cavities in the ferrite are supposed to be spherical in shape. In § 19 we also discussed the justification of this assumption in our case.

c) The porosity p is supposed to be so small that the distortion of the field by a given cavity is practically zero at the distance where on the average the neighbouring cavities are located. The effects

of the different cavities on the field are then essentially independent. This condition is also inherent in Maxwell's law of mixtures which we used in § 19 and which led to satisfactory results for the g -values there. It is best realized for ferrite IV B ($p = 11.0$ per cent), least for ferrite IV E ($p = 29.5$ per cent).

§ 21. *Estimate of the line width.* If in a piece of ferrite without cavities a homogeneous magnetic field H_0 acts in the z -direction, then the modification of this field produced by a spherical cavity of radius a can be described outside the cavity as the field \mathbf{h} of a dipole, located at the centre of the cavity and having a magnetic moment opposite to the direction of H_0 equal to

$$m = -4\pi\mu_0 a^3 \frac{H_0 M_0'}{3\mu_0 H_0 + 2M_0'} \quad (7.1)$$

where M_0' is the magnetization at the field strength H_0 in the ideal ferrite. If we employ polar coordinates r, ϑ with the centre of the sphere as origin and the z -axis as polar axis, then the components of the field due to the dipole (7.1) in the xz -plane are

$$h_x = -\frac{3m \sin \vartheta \cos \vartheta}{4\pi\mu_0 r^3}, \quad h_z = -\frac{m(1 - 3 \cos^2 \vartheta)}{4\pi\mu_0 r^3}, \quad r \geq a. \quad (7.2)$$

In view of the roughness of our estimate we shall henceforth restrict ourselves to terms linear in m and we thus find that the total field strength at a point outside the cavity is simply $H_0 + h_z$.

We next inquire in what fraction of the volume occupied by the ferrite the field h_z has a value between h_z and $h_z + dh_z$. To make this problem definite we imagine the cavities to have equal radii and to be arranged in a cubical array. Then we may take each cavity as surrounded by a concentric cube of such size that the ratio of the volume of the cavity to that of the cube just corresponds to the porosity of the ferrite. It is in this cube that the volume fraction in question must be determined. Since the orientation of the cube with respect to the field H_0 may be chosen at random, it seems reasonable to average over all orientations of the cube.

The actual calculations were made by drawing in the xz -plane a set of curves on which the quantity

$$u = -\frac{4\pi\mu_0 a^3}{m} h_z = \frac{3\mu_0 H_0 + 2M_0'}{H_0 M_0'} h_z = \left(\frac{a}{r}\right)^3 (1 - 3 \cos^2 \vartheta) \quad (7.3)$$

has a constant value (see fig. 36) and by computing the volume of the solid obtained by revolving a zone between two adjacent curves

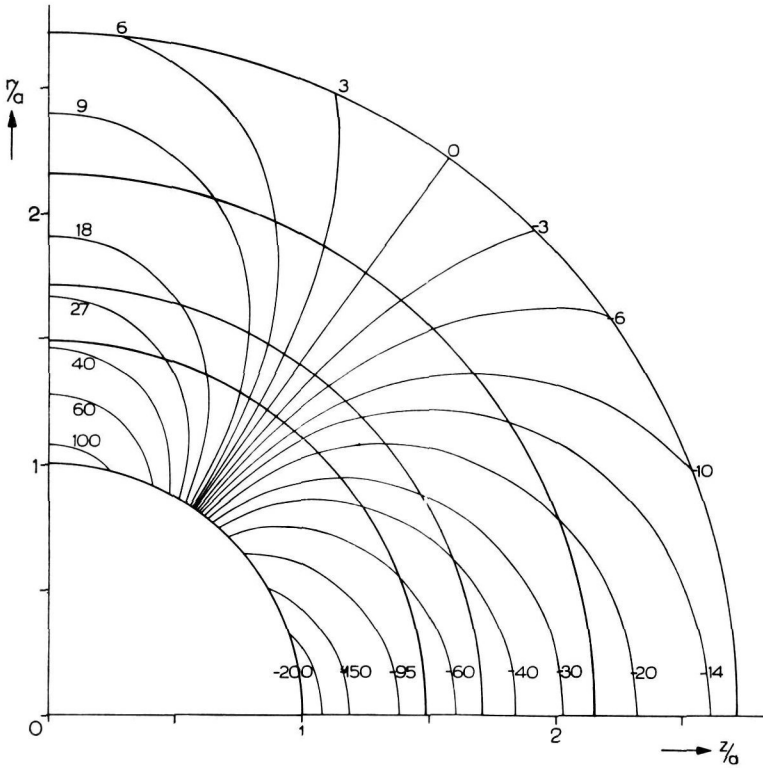


Fig. 36. Curves of constant u around a spherical cavity. The values of u are found by dividing the numbers at the curves by 125.

around the z -axis. Proper weights must be given to those parts of the zones (between the inscribed and the circumscribed sphere of the cube) which do not fall inside the cube for every orientation of the latter. The probability $P(u) du$ of u lying between u and $u + du$ is then a function of the porosity p only.

In fig. 37 the function $P(u)$ is shown for $p = 16$ per cent. The curve is asymmetrical and has a halfwidth (width at half the height of the maximum) $\Delta u = 0.26$. We compare this theoretical curve with experimental data for the ferrite IVC for which p has the

same value. According to (7.3)

$$\Delta h_z = \frac{H_0 M_0'}{3\mu_0 H_0 + 2M_0'} \Delta u. \quad (7.4)$$

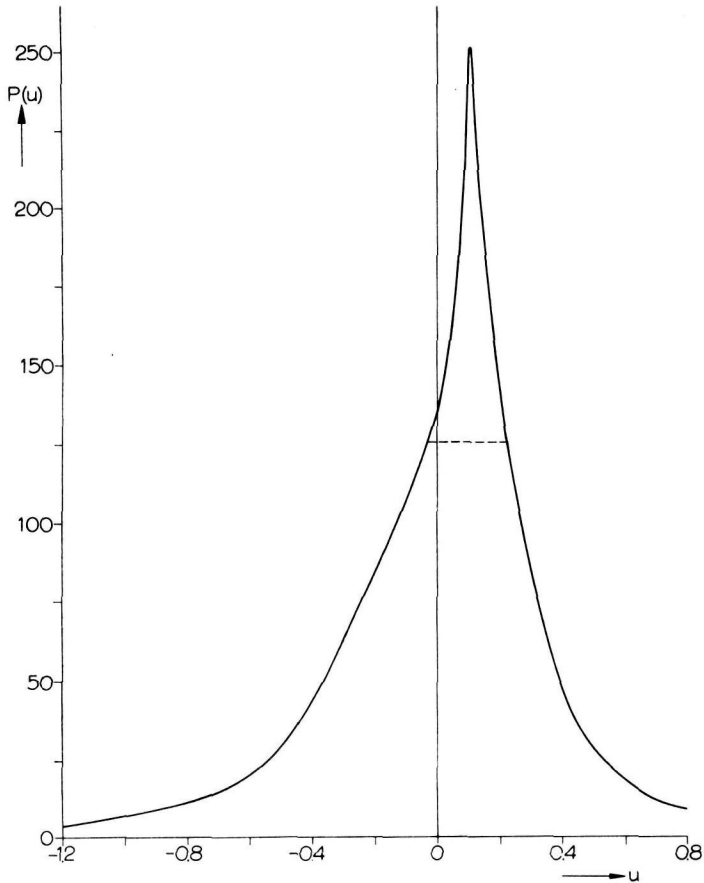


Fig. 37. The function $P(u)$. The ordinate is in arbitrary units.

For a linear medium where all the field strengths are proportional we then would have for the external field from (7.4)

$$\Delta H_{0e} = \frac{H_{0e} M_0'}{3\mu_0 H_0 + 2M_0'} \Delta u.$$

If we now make use of (6.4) to express M_0' in terms of the magneti-

zation M_0 of the porous ferrite and of (6.1) to express H_0 in terms of H_{0e} , we finally get

$$\Delta H_{0e} = \frac{H_{0e}(3\mu_0 H_p + M_0)}{3\mu_0(H_{0e} + 2H_p) + M_0} \Delta u. \quad (7.5)$$

With the values of $H_{0e} = H_r$, H_p and M_0 at resonance for $\lambda = 3.2$ cm and $T = -40$ and 20°C (see table V) and with the value of Δu given above we find from (7.5) values of ΔH_{0e} of 292 and 275 oerstedt respectively. The experimental values which we obtained with the Pound equipment¹⁴⁾ referred to in table III at the end of § 14 are 521 and 458 oerstedt respectively. For $\lambda = 1.25$ cm and $T = 20^\circ\text{C}$ the theoretical and experimental values are 378 and 845 oerstedt.

Similar calculations can be made for other values of the porosity. They show that the line width for a material of given composition and for a given wavelength and temperature is approximately proportional to the porosity, in qualitative conformity with the empirical results shown in table III of § 14.

We may hence conclude that certainly a large part of the line width is accounted for by the porosity broadening. The many approximations in our estimate make it impossible at this stage to decide whether additional mechanisms of broadening are operative besides the one considered.

§ 22. *The damping constant κ .* In the discussion of the Faraday rotation experiments in Chapter V we introduced a damping constant κ to account formally for our results. It is clear that just as the resonance in spheres of ferrite the phenomena considered there will be affected by porosity broadening. We found in particular (see fig. 30) that κ increased markedly with porosity, and this is quite in line with our expectations. Here too, however, a more quantitative interpretation would require a very careful analysis of the influence of the cavities in the ferrites as dependent on their size, shape and spatial distribution.

REFERENCES

- 1) Van Trier, A. A. T. M., Thesis Delft, 1953; Appl. Sci. Res. **B3** (1953) 142, 305.
- 2) Suhl, H. and L. R. Walker., Bell. Syst. Techn. J. **33** (1954) 1133.
- 3) Bozorth, R. M., Ferromagnetism, Van Nostrand Comp. Inc., N.Y., 1951, p. 270.
- 4) Okamura, T., Sci. Rep. Inst. Tôhoku Univ. **6A** (1954) 89.
- 5) Spencer, E. G. and R. L. Le Craw., J. Appl. Phys. **26** (1955) 250.
- 6) Saunders, W. K., I.R.E. Conv. Rec. **3** (1955) 8, 81.
- 7) Landau, L. and E. Lifshitz, Phys. Z. USSR **8** (1935) 153.
- 8) Kittel, C., Phys. Rev. **73** (1948) 155.
- 9) Van Vleck, H. J., Phys. Rev. **78** (1950) 266.
- 10) Polder, D., Phys. Rev. **73** (1948) 1116.
- 11) Kittel, C., Phys. Rev. **76** (1949) 743.
- 12) Kojima, Y., Sci. Rep. Inst. Tôhoku Univ. **6A** (1954) 614.
- 13) Maxwell, C., Treatise on electricity and magnetism, Vol. 1, Oxford, 1873, p. 365.
- 14) Beljers, H. G., Philips Res. Rep. **13** (1958) 10.

SAMENVATTING

In dit proefschrift is voor een golflengte van 3,2 cm een experimentele en theoretische studie gemaakt van de voortplanting der TE_{11} golf in een ronde golfgeleider, waarin zich een concentrisch rond staafje ferroxcube IV bevindt, dat door een statisch magneetveld in de lengterichting is gemagnetiseerd. Voor een staafje ferroxcube van bekende lengte werd de faradayrotatie en de ellipticiteit van de golf bepaald als functie van de sterkte van het statisch magneetveld met inbegrip van het ferromagnetische resonantiegebied over een temperatuurinterval van -30°C tot 100°C . Teneinde het experimentele resultaat te kunnen vergelijken met de theorie, die uitsluitend uitgewerkt is voor kleine staafdiameters, zijn deze metingen voor verschillende staafdiameters gedaan en werd de experimentele magnetische veldsterkte voor resonantie geëxtrapoleerd voor verdwijnende diameter.

Uitgaande van de theorie der ferromagnetische resonantie met demping zijn de elementen van de gyromagnetische permeabiliteitstensor berekend. Met behulp hiervan kunnen de rotatiehoek en de ellipticiteit worden uitgedrukt in de hoekfrequentie van de golf, de straal van de golfgeleider, de straal en de lengte van het ferrietstaafje, de statische magnetische veldsterkte, de statische magnetisatie, de gyromagnetische verhouding en de dempingsconstante. De gyromagnetische verhouding werd bepaald met behulp van resonantiemetingen aan bolletjes van hetzelfde ferriet, terwijl de dempingsconstante zodanig gekozen is, dat de beste overeenstemming tussen theorie en experiment is verkregen. De berekende en experimentele waarden van de resonantieveldsterkte vertoonden een bevredigende overeenstemming. De gemeten gyromagnetische verhouding en halfwaardebreedte der resonantiekromme bleken sterk afhankelijk te zijn van de temperatuur en de golflengte. Met behulp van de porositeitsinvloed kon deze afhankelijkheid worden verklaard.

CURRICULUM VITAE

Jan Snieder werd op 7 Juli 1928 te Edam geboren en volgde aldaar het lager onderwijs van 1935 tot 1941, en daarna het vierjarig MULO onderwijs dat met het B-examen in 1945 werd afgesloten. Hij werd toen tot de vierde klas der H.B.S. *B* te Amsterdam toegelaten, op welke school het eindexamen in 1947 werd verkregen.

Door middel van een renteloos voorschot werd zijn studie aan de Gemeente-Universiteit van Amsterdam mogelijk gemaakt. Het candidaatsexamen *a* in de Faculteit der Wis- en Natuurkunde legde hij in October 1950 af. Vervolgens koos hij de studierichting experimentele natuurkunde, waarbij twee en een half jaar op het Laboratorium voor Massaspectrografie onder leiding van Dr. J. Kistemaker werd gewerkt aan electromagnetische gasontladingen. De inkomsten van een leraarsbetrekking aan een avondschool en een kleine studietoelage maakten het hem toen mogelijk verder te studeren zonder renteloos voorschot.

Na het beëindigen van het praktische gedeelte van zijn studie vervulde hij zijn militaire dienstplicht van Juni 1953 tot April 1955. Na een basisopleiding werd hij als officier gedetacheerd op het Fysisch Laboratorium der Rijksverdedigings Organisatie-T.N.O. Tijdens zijn militaire diensttijd heeft hij zijn studie beëindigd en het doctoraal examen afgelegd in December 1954. Van 1955 tot heden was hij in burgerverband werkzaam op laatstgenoemd laboratorium, alwaar o.a. de in dit proefschrift beschreven metingen werden verricht.

STELLINGEN

I

Een verkleining van de porositeit van ferrieten maakt het praktisch gebruik van de faradayrotatie in een golfgeleider mogelijk bij langere golflengten.

II

De invloed van de dikte van een concentrische ferrietstaaf op de resonantievelddsterkte bij het faradayeffect in een ronde golfgeleider heeft dezelfde oorzaak als de invloed van de straal van een ferrietbolletje op de effectieve g-waarde.

Yager, W. A. and F. R. Merritt, *Phys. Rev.* **81** (1951) 477.

III

Door het meten van de aanvangspermeabiliteit, de resonantie-halfwaardebreedte en de magnetisatie van nikkelferriet met verschillende porositeit kunnen inlichtingen worden verkregen omtrent de fysische oorzaak van de ferromagnetische resonantieverliezen.

IV

De tot nog toe afgeleide formules voor de faradayrotatie kunnen niet gebruikt worden om de frequentie-afhankelijkheid van de praktische toepassingen daarvan met behulp van dikke cilindervormige ferrietstaafjes te berekenen.

V

Voor sommige systematische onderzoeken aan materialen in golfgeleiders bij temperaturen van -40°C tot kamertemperatuur heeft het gebruik van een compressor-type koelmachine praktische en economische voordelen boven het gebruik van vloeibare lucht.

VI

Er zijn aanwijzingen, dat het superhoogvacuum-gebied (10^{-8} - 10^{-12} mm Hg) binnenkort van technisch belang zal zijn.

VII

Het experimentele resultaat van Murray, dat de potentiaal in het plasma van electromagnetische gasontladingen negatief is, moet in tegenstelling tot zijn eigen opvatting aanvaard worden.

- Murray, R., Methods of study of arc discharges in uniform magnetic fields. Proefschrift Oak Ridge Nat. Lab. (1950).
Veenstra, P. C. and J. M. W. Milatz, *Physica* **16** (1950) 528.
Kistemaker, J. and J. Snieder, *Physica* **19** (1953) 950.

VIII

Bij het nauwkeurig meten van dielectrische constanten met behulp van de impedantiemethode van von Hippel dient op iedere golflengte de lege meetcellengte te worden gecorrigeerd voor de mogelijke parasitaire reflecties in de golfgeleider tussen de antenne van de meetdetector en de plaats van het te meten monster.

- von Hippel, A. R., Dielectric materials and applications. John Wiley and Sons Inc. N.Y. (1954) blz. 67.
de Vos, F. C., The experimental determination of dielectric properties at frequencies between 50 c/s and 5000 Mc/s. Proefschrift Leiden (1958) blz. 90.

IX

Ter vergroting van de veiligheid van het huidige verkeer zou het aanbeveling verdienen artikel 23 van het wegenverkeersreglement te wijzigen ten aanzien van het passeren door het langzaam verkeer van het snelverkeer.

X

Het is onbillijk dat ongehuwden boven een bepaalde leeftijd over dezelfde inkomsten zoveel meer belasting moeten betalen dan gehuwden zonder kinderen.